Atmos. Chem. Phys., 16, 12897–12924, 2016
www.atmos-chem-phys.net/16/12897/2016/
doi:10.5194/acp-16-12897-2016

Atmospheric Chemistry and Physics Open Access EGU

Current understanding of the driving mechanisms for spatiotemporal variations of atmospheric speciated mercury: a review

Huiting Mao[1], **Irene Cheng**[2], **and Leiming Zhang**[2]

[1]Department of Chemistry, State University of New York College of Environmental Science and Forestry, Syracuse, NY 13210, USA
[2]Air Quality Research Division, Science and Technology Branch, Environment and Climate Change Canada, Toronto, M3H 5T4, Canada

Correspondence to: Huiting Mao (hmao@esf.edu)

Received: 16 July 2016 – Published in Atmos. Chem. Phys. Discuss.: 21 July 2016
Revised: 16 September 2016 – Accepted: 29 September 2016 – Published: 19 October 2016

Abstract. Atmospheric mercury (Hg) is a global pollutant and thought to be the main source of mercury in oceanic and remote terrestrial systems, where it becomes methylated and bioavailable; hence, atmospheric mercury pollution has global consequences for both human and ecosystem health. Understanding of spatial and temporal variations of atmospheric speciated mercury can advance our knowledge of mercury cycling in various environments. This review summarized spatiotemporal variations of total gaseous mercury or gaseous elemental mercury (TGM/GEM), gaseous oxidized mercury (GOM), and particulate-bound mercury (PBM) in various environments including oceans, continents, high elevation, the free troposphere, and low to high latitudes. In the marine boundary layer (MBL), the oxidation of GEM was generally thought to drive the diurnal and seasonal variations of TGM/GEM and GOM in most oceanic regions, leading to lower GEM and higher GOM from noon to afternoon and higher GEM during winter and higher GOM during spring–summer. At continental sites, the driving mechanisms of TGM/GEM diurnal patterns included surface and local emissions, boundary layer dynamics, GEM oxidation, and for high-elevation sites mountain–valley winds, while oxidation of GEM and entrainment of free tropospheric air appeared to control the diurnal patterns of GOM. No pronounced diurnal variation was found for Tekran measured PBM at MBL and continental sites. Seasonal variations in TGM/GEM at continental sites were attributed to increased winter combustion and summertime surface emissions, and monsoons in Asia, while those in GOM were controlled by GEM oxidation, free tropospheric transport, anthropogenic emissions, and wet deposition. Increased PBM at continental sites during winter was primarily due to local/regional coal and wood combustion emissions. Long-term TGM measurements from the MBL and continental sites indicated an overall declining trend. Limited measurements suggested TGM/GEM increasing from the Southern Hemisphere (SH) to the Northern Hemisphere (NH) due largely to the vast majority of mercury emissions in the NH, and the latitudinal gradient was insignificant in summer probably as a result of stronger meridional mixing. Aircraft measurements showed no significant vertical variation in GEM over the field campaign regions; however, depletion of GEM was observed in stratospherically influenced air masses. In examining the remaining questions and issues, recommendations for future research needs were provided, and among them is the most imminent need for GOM speciation measurements and fundamental understanding of multiphase redox kinetics.

1 Introduction

Atmospheric mercury (Hg) is a pervasive toxic with comparable natural and anthropogenic sources (UNEP, 2013). It is operationally defined in three forms, gaseous elemental mercury (GEM), gaseous oxidized mercury (GOM), and particulate-bound mercury (PBM). In most environments GEM comprises > 95 % of total gaseous mercury (TGM =

GEM+GOM) with lifetime of 0.5–1 year (Driscoll et al., 2013). Besides emissions, GOM and PBM are largely formed from oxidation of GEM, with lifetimes of hours to weeks (Cole et al., 2014). They are highly soluble, and their wet and dry deposition is a major input of Hg to ecosystems and oceans followed by bioaccumulation, where Hg can enter human bodies through the food chain. To ultimately regulate anthropogenic emissions of Hg in order to control the ambient atmospheric concentration of Hg, it is imperative to understand Hg cycling between the atmosphere, ecosystems, and oceans.

The pathways of Hg cycling include chemical transformation and transport via air and water in various systems as illustrated in Subir et al. (2011). Mercury can be chemically transformed from one species to another through oxidation/reduction reactions, complex formation, phase transitions, biodegradation, and surface and heterogeneous interactions with aerosols, clouds, snow, and ice. Mercury can also be redistributed between geographic locations and spheres through physical processes such as wind, water runoff, dry and wet deposition, and volatilization. In addition, natural and anthropogenic sources of Hg are distributed vastly unevenly as a result of anthropogenic activities and land surface types. The eventual effect of all these processes, some of which are in fact sinks and sources, is manifested in the great heterogeneity of temporal and spatial variations of atmospheric Hg concentrations observed in numerous studies (Sprovieri et al., 2010b, references therein; references in Tables S1–S7 in the Supplement). Characterization and intercomparison of such variations for different geographic and chemical environments can provide a gateway to our understanding of Hg cycling.

Numerous measurement studies in the literature have shown distinctly different spatiotemporal variations of GEM, GOM, and PBM in the following environments, owing to their respective atmospheric chemical composition, sources, and meteorological conditions:

- marine boundary layer (MBL);
- land: urban, rural, and remote;
- high elevation, high altitude;
- low, mid-, and high latitudes.

Such differences were attributed to natural and anthropogenic sources of not only Hg but also other reactive chemical compounds that are involved in Hg cycling, meteorological conditions, and chemistry, all of which were highly dependent on geographic locations and surrounding land surface types. Therefore, it is highly complex to delineate the effects of controlling factors determining observed spatiotemporal variations of Hg concentrations.

Sprovieri et al. (2010b) reviewed the state of global mercury measurements focusing on instrumentation and techniques, and ranges of concentration levels in studies from different continents and oceanic regions up to 2009. Atmospheric Hg research has since continued to flourish, and in particular longer datasets accumulated in several regions have become available for temporal variability characterization, as to understand the driving mechanisms for such variabilities. Also of importance is the efficacy of emission reductions that have been implemented in North America and Europe for nearly 2 decades and over shorter periods in East Asia. This paper, different from Sprovieri et al. (2010b), aimed to provide a global picture of spatiotemporal variations of speciated Hg using measurement-based studies in the literature over ocean, over land, by altitude, and by latitude, and further glean insight on important factors that could potentially contribute to the observed variations.

It should be noted that units were converted for a standard atmosphere for comparison. One more cautionary note is that Hg data in earlier studies had coarser temporal resolution than in more recent studies, and hence the comparisons should be viewed with this caveat in mind. Though the earlier studies tended to have orders of magnitude larger concentrations, suggesting at higher temporal resolution those concentrations would have been even larger.

2 Marine boundary layer

Measured TGM/GEM, GOM, and PBM concentrations in the MBL globally were summarized in Tables S1–S3 of the Supplement. Spatiotemporal variations in speciated Hg were summarized with respect to their ambient concentration levels, continental (including anthropogenic) influence, hemispheric gradient, diurnal to annual cycles, and long-term trends, accompanied by discussions on potential causal mechanisms.

2.1 TGM/GEM

TGM and GEM in the MBL have been measured since the late 1960s. Near the surface in most environments, except polar springtime and Dead Sea mercury depletion events (MDEs) when strong GEM oxidation occurs, the difference between TGM and GEM was small to negligible (e.g., Temme et al., 2003a; Mao and Talbot, 2012). Concentrations were generally higher in near-coastal regions due largely to anthropogenic influence, which under certain meteorological conditions could extend to even open oceans. Natural emissions including biomass burning, volcanic, and oceanic emissions were suggested to be of influence in some studies. It was also found that meteorological conditions could play important roles in determining ambient concentrations of TGM/GEM via transport, planetary boundary layer (PBL) dynamics, and solar radiation, especially in regions nearing emission sources such as the Mediterranean and in springtime polar regions. Long-term trends have varied over different time periods, speculated to be associated with changing

anthropogenic emissions, legacy emissions, and photooxidation.

2.1.1 Concentration metrics

The mean concentrations of TGM/GEM observed over varying time periods reported from the literature ranged from 1.05 ng m^{-3} over the Antarctic Ocean to 2.34 ng m^{-3} over the western Pacific seas, as shown in Table S1 (references therein). The concentration averaged for each oceanic region calculated using the values reported from all the studies was the lowest at 1.53 ng m^{-3} over the Antarctic Ocean and the largest at 2.36 ng m^{-3} over the western Pacific seas (Fig. 1a). The range of 0.05–29 ng m^{-3} over the Atlantic (Fig. 1a), obtained from individual studies, appeared to be the largest, although the maximum concentration was from a single event influenced by forest fires in Québec, Canada, at a long-term site in the MBL 20 km from the coast of southern New Hampshire, USA (Mao and Talbot, 2012). With that single event removed, the TGM/GEM concentrations were much more variable in the MBL of the Mediterranean Sea and its nearby seas (Table S1; references therein).

Atmospheric Hg over the Atlantic Ocean has been studied most extensively compared to other oceans, largely via shipboard measurements. Concentrations of TGM/GEM ranged from 0.05 ng m^{-3} (15 min average) in Cape Point, South Africa (Brunke et al., 2010), to 29 ng m^{-3} (5 min average) near the shore of southern New Hampshire, USA (Mao and Talbot, 2012). In the earliest shipboard global study of atmospheric Hg, Seiler et al. (1980) found highly variable TGM concentrations (1–10 ng m^{-3}, 2–4 h average) averaged at 2.8 ng m^{-3} between Hamburg (54° N, 10° E) and Santo Domingo (20° N, 67° W) across the Atlantic Ocean over 11 October–1 November 1973. It should be noted that early studies used very different measurement techniques and hence the magnitude needs to be considered with discretion. During the following 40 years, most studies reported TGM/GEM ranging from below the limit of detection (LOD) to a few ng m^{-3} and higher concentrations in near-coastal regions (Table S1; references therein). The first measurements of Hg species was a 1 month shipboard study over the South Atlantic Ocean during polar summer (February) 2001 by Temme et al. (2003b). Their measurements (5–15 min average data) during the cruise from Neumayer to Punta Arenas exhibited very small variation with TGM averaged at 1.1 ± 0.2 ng m^{-3} and no significant difference between TGM and GEM. Relatively homogeneous distributions of TGM/GEM were observed over open waters in the South Atlantic with mean values hovering around 1 ng m^{-3} and standard deviation < 0.3 ng m^{-3} compared to larger mean values (1.3–$\sim$ 3 ng m^{-3}) over the North Atlantic.

Over the Pacific Ocean, 1 to 15 min TGM/GEM concentrations measured over the North and South Pacific Ocean ranged from 0.3 ng m^{-3} over 40–45° N in July–September 2008 (Kang and Xie, 2011) to 7.21 ng m^{-3} in the Port of Los Angeles on 27 May 2010 (Weiss-Penzias et al., 2013), with generally higher concentrations near coasts and lower ones over open oceans (Table S1; reference therein). The distribution of TGM/GEM over the South Pacific appeared to be quite heterogeneous, where Xia et al. (2010) measured TGM averaged at 2.20 ± 0.67 ng m^{-3}, a factor of 2 higher than those in Soerensen et al. (2010), who measured a mean of 1.03 ± 0.16 ng m^{-3}.

Over the South China Sea, the Yellow Sea, and other neighboring seas, located on the eastern Asian continental margin in the tropical–subtropical western North Pacific, elevated concentrations of TGM/GEM were observed with mean values varying over 2.08–2.62 ng m^{-3} (Fu et al., 2010b; Nguyen et al., 2011; Ci et al., 2011) (Table S1). TGM concentrations over the Mediterranean Sea, Adriatic Sea, Dead Sea, Augusta Basin, and Baltic Sea ranged from 0.4 to 11 ng m^{-3} (Table S1; references therein).

A few studies on Hg over the Indian Ocean (Soerensen et al., 2010; Xia et al., 2010; Witt et al., 2010a; Angot et al., 2014) reported a concentration gradient of TGM with increasing concentrations at more northern locations closer to the inter-tropical convergence zone (ITCZ), with a mean concentration of 1.24 ± 0.06 ng m^{-3} over 9–21° S latitudes (Witt et al., 2010a).

Studies on TGM/GEM over the Arctic Ocean showed fairly constant concentrations in January and August–December and reported MDEs in spring and summertime annual maximums (Lindberg et al., 2002; Aspmo et al., 2006; Sommar et al., 2010; Steffen et al., 2013; Yu et al., 2014). During the 1998–2001 Barrow Atmospheric Mercury Study (BAMS), daily average GEM concentrations ranged from < 0.2 to $\sim$ 3.7 ng m^{-3}, averaged between 1.5 and 2 ng m^{-3} in January and mid-August–December (Lindberg et al., 2002). The means and ranges measured in summer 2004, 2005, and 2012 (Aspmo et al., 2006; Sommar et al., 2010; Yu et al., 2014) were well within the 1999 summertime range of Lindberg et al. (2002) (Table S1). Different concentrations of GEM over sea ice–covered (1.81 ± 0.43 ng m^{-3}) vs. sea ice-free (1.55 ± 0.21 ng m^{-3}) Arctic Ocean waters were measured by Sommar et al. (2010) in summer 2005. In spring 2009 (14–26 March) a mean 5 min GEM concentration of 0.59 ng m^{-3} was measured with a range of 0.01–1.51 ng m^{-3} over sea ice on the Beaufort Sea near Barrow, Alaska, which appeared to be depleted compared to annual Arctic ambient boundary layer concentrations (Steffen et al., 2013).

In Antarctica, the first study, conducted by de More et al. (1993), reported a mean TGM concentration of 0.55 ± 0.28 ng m^{-3} and a range of 0.02–1.85 ng m^{-3} (24–48 h) at Ross Island during 1987–1989. Over November 2000–January 2001, Sprovieri et al. (2002) reported a similar range but a mean of 0.9 ± 0.3 ng m^{-3}, twice as large than that of de More (1993) a decade earlier. Similar means and ranges of TGM/GEM concentrations were measured by Ebinghaus et al. (2002b), Temme et al. (2003b), Soerensen et al. (2010), and Xia at al. (2010). Similar mean values but

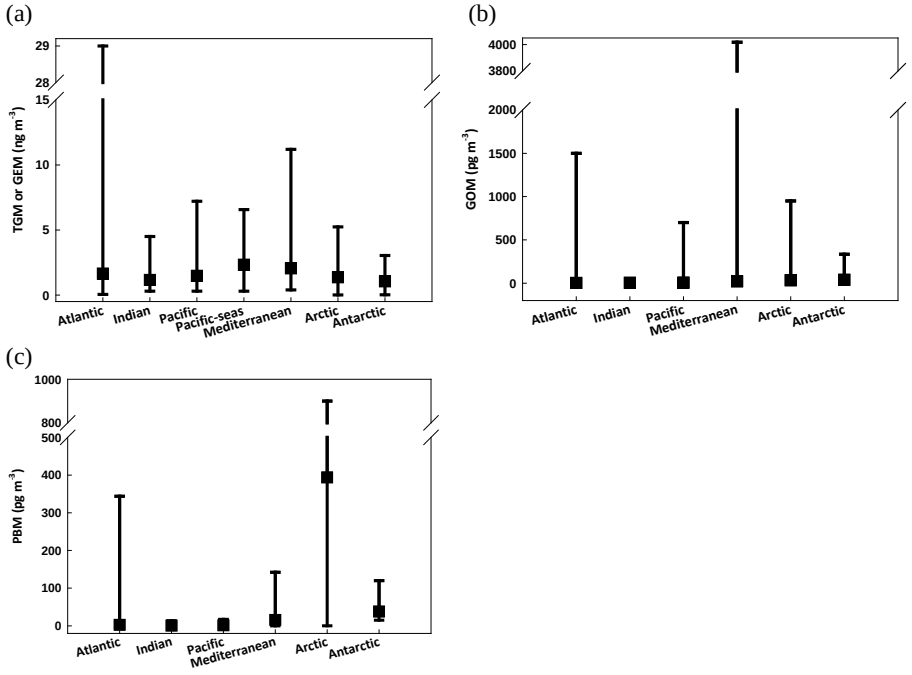

Figure 1. Means and ranges of TGM/GEM **(a)**, GOM **(b)**, and PBM **(c)** concentrations, estimated from the values in the literature as shown in Tables S1–S3, over the Atlantic, Indian, Pacific, seas over the western Pacific (denoted as Pacific-Seas, only TGM/GEM in this category), seas in the Mediterranean region (denoted as Mediterranean), Arctic, and Antarctica Ocean. The solid black squares represent the mean value and the lowest whisker the minimum and the largest the maximum concentration in the region.

a much wider range (0.02–3.07 ng m^{-3}) were found in the multi-year dataset in Pfaffhuber et al. (2012) (Table S1).

2.1.2 Hemispheric difference

Hemispheric gradient over the Atlantic and Pacific oceans has been reported since the 1980s, with higher concentrations in the North Atlantic attributed to anthropogenic and biomass burning emissions (Seiler et al., 1980; Slemr et al., 1981, 1985, 1995; Slemr and Langer, 1992; Fitzgerald et al., 1996; Lamborg et al., 1999; Temme et al., 2003a; Chand et al., 2008; Xia et al., 2010; Soerensen et al., 2010; Müller et al., 2012). An average gradient of 0.37 ng m^{-3} in TGM was measured in October–November 1973 (Seiler et al., 1980). Measurements from the same cruise paths from Hamburg (54° N) to Buenos Aires (35° S) in 1977, 1978–1980, 1992, and 1994 consistently showed TGM hemispheric difference, 1.56 ± 0.32 and 1.05 ± 0.22 ng m^{-3} in the Northern Hemisphere (NH) and Southern Hemisphere (SH), respectively, in 1977, increased to 2.25 ± 0.41 and 1.50 ± 0.30 ng m^{-3} in 1992 followed by significant decreases to 1.79 ± 0.41 and 1.18 ± 0.17 ng m^{-3} in 1994 (Slemr et al., 1981, 1985, 1995; Slemr and Langer, 1992). The hemispheric difference from a NH average of 1.32 ± 0.16 ng m^{-3} in summer 2006 and 2.61 ± 0.36 ng m^{-3} in spring 2007, and a SH average of 1.27 ± 0.2 ng m^{-3} measured by Soerensen et al. (2010) was close to the 1978–1980 hemispheric gradient in Slemr et al. (1985) but lower than the 1990 value in Slemr and Langer (1992).

Over the Pacific a hemispheric gradient of ~ 0.4 ng m^{-3} was found in early studies by Seiler et al. (1980) and Fitzgerald et al. (1984). Higher concentrations but similar magnitude of hemispheric difference of TGM was measured in December 2007 by Xia et al. (2010) with a mean of 1.746 ± 0.513 ng m^{-3} over the North Pacific and 1.471 ± 0.842 ng m^{-3} over the southern Indian Ocean (note: their cruise passed through the southern Indian Ocean instead the South Pacific). Around the same time, Soerensen et al. (2010) measured nearly twice lower concentrations over the South Pacific (1.11 ± 0.11 ng m^{-3} along the Chilean Coast and up to 1.33 ± 0.24 ng m^{-3} near East Australia) than the North Atlantic concentrations (mean values of 2.26 and 2.86 ng m^{-3} over 23–59° N; no measurements over the North Pacific in the study) from the same study.

Studies found higher TGM concentrations up to ~ 2.3 ng m^{-3} over the equatorial Pacific in October 1980, markedly higher (> 0.5 ng m^{-3}) than those outside this region (Fitzgerald et al., 1984; Kim and Fitzgerald, 1988). However, Wang et al. (2014) found no sustained high-GEM concentrations indicative of persistently enhanced biotic mercury evasion from the upwelling region over the Galápagos Islands in the equatorial Pacific during February–October 2011. They found GEM concentrations

averaged at $1.08 \pm 0.17\,\mathrm{ng\,m^{-3}}$, 2 times lower than the earlier ones.

2.1.3 Temporal variations from diurnal cycle to long-term trend

Diurnal variation

Early studies on TGM over the Atlantic Ocean showed 1 order of magnitude larger diurnal amplitude than that in more recent studies, with daily peaks of $5\,\mathrm{ng\,m^{-3}}$ at noon and amplitude of 2–3 $\mathrm{ng\,m^{-3}}$ across the North and South Atlantic in Seiler et al. (1980). Yet none was observed by Slemr et al. (1981, 1985) and Slemr and Langer (1992). Measurements of TGM at Cape Point, South Africa (Brunke et al., 2010) and GEM at Appledore Island, Maine, USA (Mao and Talbot, 2012), exhibited pronounced diurnal variation in summer with daily peaks (minimums) before sunrise (in the late afternoon) and amplitudes of $0.8\,\mathrm{ng\,m^{-3}}$ and ~ 10 ppqv ($\sim 0.09\,\mathrm{ng\,m^{-3}}$) for the two sites, respectively.

The opposite diurnal pattern with significant amplitude was observed over the Pacific (Fitzgerald et al., 1984; Weiss-Penzias et al., 2003, 2013; Kang and Xie, 2011; Tseng et al., 2012; Wang et al., 2014) with daily peaks ranging from $0.7\,\mathrm{ng\,m^{-3}}$ (5 min) over the Japan Sea (Kang and Xie, 2011) to $2.25\,\mathrm{ng\,m^{-3}}$ (unknown time resolution) in the equatorial region (Fitzgerald et al., 1984). The most pronounced diurnal variation in TGM was reported in Fitzgerald et al. (1984) with daily amplitude of $0.7\,\mathrm{ng\,m^{-3}}$ in the equatorial region (4° N–10° S). A similar pattern and magnitude of GEM diurnal variation was observed by Tseng et al. (2012) over the South China Sea during May 2003–December 2005, especially in warm seasons. Opposite patterns were observed in Weiss-Penzias et al. (2003, 2013). Laurier et al. (2003) found no diurnal variation during a cruise from Osaka, Japan, to Honolulu, Hawaii, over 1 May 2002–4 June 2002.

Over the Arctic diurnal variation of GEM was observed by Lindberg et al. (2002) with noontime minimums in spring and summer, diurnal amplitude $\sim 2\,\mathrm{ng\,m^{-3}}$ on a typical day in January–June. On the other hand, the shipboard measurements from Sommar et al. (2010) suggested very small near-zero diurnal variation. Similarly, no diurnal variation was found over the Antarctica (Pfaffhuber et al., 2012), except one case with influence of in situ human activity.

Seasonal to annual variation

Annual cycles of TGM/GEM were reported over the Atlantic in both hemispheres. Annual cycles with an annual maximum in austral summer and a minimum in austral winter and average amplitude of $0.134\,\mathrm{ng\,m^{-3}}$ were observed at Cape Point, South Africa (Slemr et al., 2008; Brunke et al., 2010). Opposite annual variation with higher (lower) concentrations in winter (summer) was measured over the North Atlantic, such as Mace Head (amplitude $0.097\,\mathrm{ng\,m^{-3}}$), a remote site on the west coast of Ireland adjacent to the North Atlantic (Ebinghaus et al., 2002a) and the Appledore Island (25 ppqv, i.e., $\sim 0.2\,\mathrm{ng\,m^{-3}}$) site in Mao and Talbot (2012). Similarly, significant seasonal variation in NH with an annual minimum in July and maximum in January–March and amplitude of 0.3–0.4 $\mathrm{ng\,m^{-3}}$ was measured in a global cruise (Soerensen et al., 2010).

Average seasonal difference of $0.19\,\mathrm{ng\,m^{-3}}$ GEM concentrations over the Pacific were observed by Wang et al. (2014) with the highest and most variable concentrations over February–May 2011 and the lowest and least variable in October over the Galápagos Islands during 12 November 2011–11 December 2011. In contrast, a lack of seasonal variation in GEM was reported by Weiss-Penzias et al. (2003) using a subset of data of marine origin extracted from 1 year speciated Hg data (May 2001–May 2002) at the Cheeka Peak Observatory on the east coast of the Pacific. This was uncharacteristic of midlatitudinal NH sites, but significant interannual variation was noted in this study.

Distinct annual variation in GEM over the South China Sea was observed in the cruise study by Tseng et al. (2012) over May 2003–December 2005. The winter maximum was $5.7 \pm 0.2\,\mathrm{ng\,m^{-3}}$ and summer minimum $2.8 \pm 0.2\,\mathrm{ng\,m^{-3}}$, 2–3 times higher than global background levels. Difference of $0.4\,\mathrm{ng\,m^{-3}}$ in seasonal average GEM was quantified with higher concentrations in the summer than in the fall over the Adriatic Sea (Sprovieri et al., 2010) and less than a factor of 2 over the Augusta Basin (Bagnato et al., 2013). The study by Obrist et al. (2011) was the first to show the occurrence of MDEs in midlatitudes with GEM down to 22 ppqv ($0.2\,\mathrm{ng\,m^{-3}}$) most frequently in summer in the boundary layer of the Dead Sea, as opposed to MDEs, as commonly known, occurring in the springtime Arctic and Antarctic only.

Annual variation of GEM over the Indian Ocean was reported in Angot et al. (2014) with higher concentrations in winter ($1.06 \pm 0.09\,\mathrm{ng\,m^{-3}}$) and lower in summer ($1.04 \pm 0.07\,\mathrm{ng\,m^{-3}}$), opposite of those at Cape Point (Slemr et al., 2008) and Galapagos Islands (Wang et al., 2014) with annual amplitude an order of magnitude smaller.

Annual maximum concentrations of GEM occurred in summer over the Arctic Ocean and frequent MDEs with GEM depleted to near zero in spring (Lindberg et al., 2002; Aspmo et al., 2006; Cole et al., 2013; Moore et al., 2013). Lindberg et al. (2002) observed GEM concentrations up to $4\,\mathrm{ng\,m^{-3}}$ in June 2000 compared to $1.82 \pm 0.24\,\mathrm{ng\,m^{-3}}$ in summer 2004 (Aspmo et al., 2006) and $1.23 \pm 0.61\,\mathrm{ng\,m^{-3}}$ in summer 2012 (Yu et al., 2014).

Seasonal variation in Antarctic Hg suggested large variation in TGM/GEM in spring due to the occurrence of MDEs. The longest continuous data record in the Antarctic started in February 2007 at the Norwegian Antarctic Troll Research Station (TRS) in Queen Maud Land near the Antarctic coast (Pfaffhuber et al., 2012). Concentrations were fairly constant hovering at $\sim 1 \pm 0.07\,\mathrm{ng\,m^{-3}}$ in late fall through winter

and highly variable ranging from 0.02 to 3.04 ng m^{-3} with a mean of 0.86 ± 0.24 ng m^{-3} in spring and summer (Pfaffhuber et al., 2012), close to the values from 6 years earlier in Sprovieri et al. (2002) and Temme et al. (2003b).

Long-term trends

Long-term trends in TGM over the Atlantic varied during different time periods of the past decades. TGM concentrations averaged over latitudes from Hamburg, Germany, to Punta Arenas, Chile, were increasing at a rate of 1.46 ± 0.17 % yr^{-1} from 1970 to 1990 (Slemr and Langer, 1992) followed by a 22 % decrease from 1990 to 1994 (Slemr et al., 1995). In similar latitudinal coverage but over a wider longitudinal span during three cruises in September–November 1996, December 1999–March 2000, and February 2001, TGM concentrations were averaged at 1.26 ± 0.1 ng m^{-3} (Temme et al., 2003a), comparable to the 1977–1980 (Slemr et al., 1985) and 1994 concentrations (Slemr et al., 1995) but lower than the 1990 ones (Slemr et al., 1992). Over September 1995–December 2001, a slight increase (4 %) in TGM was observed at Mace Head (Ebinghaus et al., 2002a). In the South Atlantic at Cape Point a small but significant decrease was reported in TGM annual median from 1.29 ng m^{-3} in 1996 to 1.19 ng m^{-3} in 2004 (Slemr et al., 2008), and at an about 3 times faster decreasing rate (-0.034 ± 0.005 ng m^{-3} yr^{-1}) over 1996–2008 (Slemr et al., 2011). A statistically significant decreasing trend of -0.028 ± 0.01 ng m^{-3} yr^{-1} ($\sim$ 1.6–2.0 % yr^{-1}) in TGM over the North Atlantic was reported for the same time period at Mace Head, Ireland (Ebinghaus et al., 2011). In an updated study, Weigelt et al. (2015) presented a relatively smaller decreasing trend of -0.016 ± 0.002 ng m^{-3} yr^{-1} in monthly median marine GEM concentrations over 1996–2013. In Soerensen et al. (2012) a steep 1990–2009 decline of -0.046 ± 0.010 ng m^{-3} yr^{-1} (-2.5 % yr^{-1}) was found in TGM over the North Atlantic (steeper than at NH land sites) but no significant decline over the South Atlantic. A recent comparison by Slemr et al. (2015) found smaller trends during shorter time periods and a possible increasing trend at Cape Point for the period 2007–2013, qualitatively consistent with the trend changes observed at Mace Head (Weigelt et al., 2015).

Over the Arctic Ocean, weak or insignificant declines in TGM at rates of -0.007 ± 0.019 and -0.003 ± 0.012 ng m^{-3} yr^{-1} were found at Alert and Zeppelin, respectively, during 2000–2009, significantly smaller than the trends at midlatitude sites (Ebinghaus et al., 2011; Slemr et al., 2011; Soerensen et al., 2012; Cole et al., 2013; Berg et al., 2013; Weigelt et al., 2015). TGM/GEM concentrations over the Antarctic Ocean appeared to have increased from the 1980s to the 2000s (Ebinghaus et al., 2002b; Temme et al., 2003b; Soerensen et al., 2010; Xia et al., 2010; Pfaffhuber et al., 2012), and no significant trend was detected over 2007–2013 (Slemr et al., 2015).

2.1.4 Mechanisms driving the observed temporal variabilities

Causes for episodic higher concentrations

It has been hypothesized that anthropogenic, biomass burning, and volcanic emissions caused higher concentrations over open waters and near-coastal regions in many cases. Such influences on the atmospheric concentration of Hg was demonstrated using backward trajectories and correlations of TGM/GEM with carbon monoxide (CO), ^{222}Rn, black carbon, sulfur dioxide (SO_2), and dimethylsulfide (DMS) (Williston, 1968; Seiler et al., 1980; Fitzgerald et al., 1984; Kim and Fitzgerald, 1988; Slemr et al., 1981, 1985; Slemr and Langer, 1992; Slemr, 1996; Lamborg et al., 1999; Sheu and Mason, 2001; Laurier and Mason, 2007; Soerensen et al., 2010; Mao and Talbot, 2012; Müller et al., 2012; Xia et al., 2010; Chand et al., 2008; Kang and Xie, 2011; Weiss-Penzias et al., 2013; Fu et al., 2010b; Nguyen et al., 2011; Ci et al., 2011; Bagnato et al., 2013; Kotnik et al., 2014). Some studies also suggested that oceanic evasion was an important source contributing to higher concentrations (Seiler et al., 1980; Pirrone et al., 2003; Sigler et al., 2009b), while others thought otherwise (Slemr et al., 1981, 1985; Slemr and Langer, 1992). Strong photoreduction could have caused higher TGM/GEM concentrations under sunny, warm and dry conditions with lower amounts of precipitation in the Mediterranean Sea region (Pirrone et al., 2003; Sprovieri et al., 2003; Sprovieri and Pirrone, 2008). These influences often occurred in multitude simultaneously leading to elevated ambient Hg concentrations.

Diurnal variation

In nearly all studies, diurnal variation over the Atlantic, Pacific, and Arctic was found to be most pronounced in warm seasons, i.e., spring and/or summer. Different combinations of oceanic emissions, photooxidation, biological production, and meteorology were suggested to work together shaping the observed patterns in different oceanic regions. The pattern with daytime peaks was attributed to oceanic emissions and biological production in sea water (Seiler et al., 1980; Fitzgerald et al., 1984; Tseng et al., 2012; Wang et al., 2014), which was supported by the concurrent measurements of dissolved elemental Hg (Tseng et al., 2012). The opposite pattern with daytime minimums was associated with photooxidation of GEM by abundant halogen radicals and meteorological conditions (Lindberg et al., 2002; Brunke et al., 2010; Mao and Talbot, 2012; Weiss-Penzias et al., 2003, 2013). The most pronounced diurnal variation in TGM in the equatorial area (4° N–10° S) was demonstrated to be caused by biological production (Fitzgerald et al., 1984).

However, Mao et al. (2012) suggested that the predominant effect of oceanic evasion on ambient GEM concentrations was episodic, not necessarily diurnal, because they

found, among all physical parameters, the only significant correlation GEM had was with wind speed exceeding $15\,m\,s^{-1}$ at a marine location, which occurred rather sparsely. This was corroborated by Sigler et al. (2009b) suggesting enhanced oceanic evasion at a rate of ~ 7 ppqv h^{-1} ($0.063\,ng\,m^{-3}$) leading to 30–50 ppqv ($0.27–0.45\,ng\,m^{-3}$) increases in coastal and inland GEM concentrations in southern New Hampshire, USA, during the April 2007 nor'easter.

In the study by Laurier et al. (2003) the lack of diurnal variation over the Pacific was speculated to be caused by continuous evasion from surface water. Over the Arctic, unlike the distinctive diurnal pattern with noontime peaks in the study by Lindberg et al. (2002), very small near-zero diurnal variation in GEM was manifested in the shipboard measurements of Sommar et al. (2010) and was speculated to result from low in situ oxidation of GEM. No diurnal variation was found over the Antarctica due possibly to lack of diurnally varying sources and sinks (Pfaffhuber et al., 2012), except one case with in situ human activity.

Seasonal to annual variation

Annual cycles of TGM/GEM in the MBL differed between various oceanic regions and were suggested to be driven predominantly by oceanic evasion, biomass burning, anthropogenic emissions, interhemispheric flux, and/or meteorological conditions (Slemr et al., 2008; Ebinghaus et al., 2002a, b; Sigler et al., 2009a; Brunke et al., 2010; Soerensen et al., 2010; Mao and Talbot, 2012; Angot et al., 2014; Wang et al., 2014). Annual cycles of TGM/GEM with an annual maximum in summer and a minimum in winter observed at Cape Point, South Africa, in the South Atlantic MBL was hypothesized to be driven predominantly by oceanic emissions, biomass burning, and anthropogenic activities (Brunke et al., 2010), and interhemispheric flux (Slemr et al., 2008; Brunke et al., 2010). Higher concentrations of GEM in the summer over the Adriatic Sea (Sprovieri et al., 2010a) and over the Augusta Basin (Bagnato et al., 2013) were suggested to be caused by stagnant meteorological conditions in the former study and enhanced evasion from sea water in the latter. Opposite annual variation with higher (lower) concentrations in winter (summer) was proposed to be determined largely by meteorology (Ebinghaus et al., 2002a, 2011) and photochemical oxidation of GEM (Mao and Talbot, 2012). The same annual cycle over the Indian Ocean was speculated to be a result of long-range transport of air masses originated from southern Africa biomass burning during the winter months (July–September), and low GEM associated with southerly polar and marine air masses from the remote southern Indian Ocean (Angot et al., 2014). Frequent MDEs in the summertime Dead Sea MBL were observed to be often concurrent with varying concentrations of bromine oxide (BrO) and high temperatures up to 45 °C (Obrist et al., 2011). Such high temperatures seemed to be contradictory to the general understanding that Br-initiated GEM oxidation tends to go forward under very cold conditions at temperature < -40 °C. Despite that, the authors suggested that Br species were the major oxidants of GEM during depletion events, even when constantly high temperatures were accompanied by sometimes low-BrO concentrations.

Springtime large variation in Arctic and Antarctic TGM/GEM was caused by the occurrence of MDEs. Polar MDEs have been generally linked to reactive Br-initiated GEM oxidation in spring when Br explosion occurs producing abundant reactive Br (Schroeder et al., 1998; Ebinghaus et al., 2002b; Lindberg et al., 2002; Temme et al., 2003b; Mao et al., 2010; Steffen et al., 2013; Moore et al., 2014). For Antarctic MDEs, Ebinghaus et al. (2002b) found a strong positive correlation between TGM and O_3 over August–October, accompanied by enhanced Global Ozone Monitoring Experiment (GOME) column BrO. Compared to Arctic MDEs, the first Antarctic MDE occurred about 1–2 months earlier, probably due to the lower latitude of the monitoring site and sea ice, the former allowing earlier sunrise and the latter conducive to Br / BrO formation. Temme et al. (2003b) found that the air masses reaching the station during MDEs had a maximum contact with sea ice (coverage $> 40\,\%$) over the South Atlantic Ocean, which was speculated to contain abundant reactive Br released from sea salt associated with sea ice or sea salt aerosols.

Summertime annual maximums of GEM over the Arctic and Antarctic oceans were generally associated with enhanced evasion of GEM and from GOM reduction in snow resulting from maximum exposed sea water after snow/ice melt (Lindberg et al., 2002; Aspmo et al., 2006; Soerensen et al., 2010; Cole et al., 2013; Moore et al., 2014), which was also suggested using model simulations by Dastoor and Durnford (2014). A different mechanism of riverine contribution was hypothesized in Fischer et al. (2012) using an atmosphere–ocean coupled model. Yu et al. (2014) observed high-TGM concentrations concurrent with low salinity, CO, and high chromophoric dissolved organic matter (CDOM) over the ice-covered central Arctic Ocean and speculated that the relatively high-CDOM concentrations associated with river runoff could enhance Hg^{2+} reduction. Moreover, they related the summer monthly variability in TGM concentrations to less chemical loss.

Long-term trends

Four hypotheses were made to explain the observed decreasing trends in TGM/GEM during the past decades. First, the global decreasing trend was caused by decreased re-emission of legacy mercury as a result of a substantial shift in the biogeochemical cycle of Hg through the atmospheric, oceans, and soil reservoirs, although exactly what may have caused this shift remained unexamined (Slemr et al., 2011). Second, the decreasing trend was linked to increasing tropospheric O_3 (Ebinghaus et al., 2011). However, this speculation was negated by the plausibility of GEM oxidation by O_3 in the at-

mosphere. Third, based on atmosphere–ocean coupled model simulations, the decreasing trend in TGM over the North Atlantic was caused by decreasing North Atlantic oceanic evasion driven by declining subsurface water Hg concentrations resulting from reduced Hg inputs from rivers and wastewater and from changes in the oxidant chemistry of the atmospheric MBL (Soerensen et al., 2012). However, Amos et al. (2014) suggested that the decrease in riverine input was too small to affect Hg concentrations in the open ocean let alone the declining trend in North Atlantic sea water Hg concentrations. Last, a 20 % decrease in total Hg emissions and 30 % in anthropogenic Hg° emissions were estimated for the period of 1990–2010, leading to the observed decreasing trends in TGM/GEM, as suggested by a most recent modeling study (Zhang et al., 2016).

2.2 GOM and PBM

2.2.1 Concentration metrics

The mean concentrations of GOM from individual studies varied from below LOD in several studies to 4018 pg m^{-3} (1 h) in the Dead Sea MBL (Obrist et al., 2011; Moore et al., 2013) (Table S2; references therein). The GOM concentration averaged for each oceanic region based on values from the literature varied from 3 pg m^{-3} over the Atlantic Ocean to 40 pg m^{-3} over the Antarctica, and the largest range 0.1–4018 pg m^{-3} was over the Mediterranean Sea and its neighboring seas (Fig. 1b). Note that the small ranges in other oceanic MBL did not necessarily indicate less variability in GOM but merely a result of limited measurement data available (Table S2; references therein).

The mean concentrations of PBM from individual studies varied from below LOD in several regions to 394 pg m^{-3} (1 h) over the Beaufort Sea (Steffen et al., 2013) (Table S3; references therein). The PBM concentration averaged for each oceanic region based on values in the literature varied from 0.6 pg m^{-3} over the Indian to 394 pg m^{-3} over the Arctic Ocean (Fig. 1c). No ranges were provided for the Arctic, Antarctic, and Indian Ocean MBL due to limited numbers of studies there. The few studies available indicated that PBM concentrations were in most cases smaller and less variable than GOM.

The earliest shipboard measurements of GOM showed dimethyl mercury (DMM) concentrations orders of magnitude larger (Slemr et al., 1981, 1985) than the total GOM concentration measured in the recent two to 3 decades. Due to the use of very different techniques in early studies, those concentrations were listed in Table S2 (references therein) but were not used for comparison with more recent studies (Table S2; references therein).

Same as GEM, GOM concentrations tended to be higher over the North than the South Atlantic and in near-coastal regions than open waters (Temme et al., 2003b; Mason et al., 2001; Sheu and Mason, 2001; Mason and Sheu, 2002; Aspmo et al., 2006; Laurier and Mason, 2007; Sigler et al., 2009b; Mao and Talbot, 2012). Hourly GOM concentrations of 1–30 pg m^{-3} over the South Atlantic Ocean from Neumayer to Punta Arenas in February 2001 (Temme et al., 2003b) were 1–2 orders of magnitude smaller than the concentrations (1.38 ± 1.30 pmol m^{-3}, i.e., $\sim 300 \pm 280$ pg m^{-3}) near Bermuda in September and December 1999 and March 2000 (Mason et al., 2001). However, at around the same time average values almost an order of magnitude smaller were reported at Bermuda (50 ± 43 pg m^{-3}, a few pg m^{-3} to 128 pg m^{-3}) (Mason and Sheu, 2002) and at a US mid-Atlantic coastal site (40 pg m^{-3}) (Sheu and Mason, 2001). In comparison, GOM concentrations were an order of magnitude smaller over the open water and at higher latitude (Aspmo et al., 2006; Laurier and Mason, 2007), comparable to those over the South Atlantic. Similar magnitude of GOM concentrations were measured at a North Atlantic near-coastal MBL site with an average of 0.4 ppqv (~ 3.6 pg m^{-3}) (0–22 ppqv, i.e., 0–196 pg m^{-3}, 2 h) during 2007–2010 (Sigler et al., 2009b; Mao and Talbot, 2012).

PBM concentrations (Table S3; references therein) were measured with an average of 1.9 ± 0.2 pg m^{-3} during the May–June 1996 South and equatorial Atlantic cruise (Lamborg et al., 1999) and 1.3 ± 1.7 pg m^{-3} (< 0.5 pg m^{-3} (LOD) to 5.2 pg m^{-3}) in Bermuda, 30–40 times smaller than the concurrent weekly averaged GOM concentrations (Mason and Sheu, 2002; Sheu, 2001). At higher North Atlantic latitudes, PBM concentrations were averaged at 2.4 pg m^{-3}, very close to the concurrent average GOM concentrations but a factor of 4 smaller varying from < LOD to 6.3 pg m^{-3} in summer 2004 (Aspmo et al., 2006). Mao and Talbot (2012) reported PBM concentrations varying from 0.09 ppqv (0.8 pg m^{-3}) in winter 2010 to 0.52 ppqv (4.6 pg m^{-3}) in summer 2010.

During the 2000s, concentrations of GOM over the Pacific decreased by around a factor of 2 from 9.5 pg m^{-3} over open waters in 2002 (Laurier et al., 2003) to around 4 pg m^{-3} at a remote Japanese site downwind of major Asian source regions in spring 2004 (Chand et al., 2008) and in the equatorial region in 2011 (Wang et al., 2014) (Table S2; references therein). The maximum concentration from a decade of studies was 700 pg m^{-3} (3 h) measured in air masses originated from upper air over the Pacific (Timonen et al., 2013), about 2 orders of magnitude larger than what Chand et al. (2008) and Laurier et al. (2003) reported. PBM concentrations over the Pacific reached up to 17 pg m^{-3}, comparable to GOM, and on average were 3 times larger downwind of East Asia (3.0 ± 2.5 pg m^{-3}) than in the equatorial Pacific MBL (Chand et al., 2008; Wang et al., 2014) (Table S3).

In the southern Indian Ocean, very low GOM and PBM concentrations were observed, averaged at 0.34 (< LOD (0.28–0.42 pg m^{-3})–4.07 pg m^{-3}) and 0.67 pg m^{-3} (< LOD – 12.67 pg m^{-3}), respectively, over 2 years from a remote location, Amsterdam Island (Angot et al., 2014). These con-

centrations were at the lower end of the range of Atlantic and the Pacific MBL measurements.

Measurements over the Mediterranean Sea and its neighboring seas generally showed much higher concentration levels than over the Atlantic, Pacific, and Indian Ocean, with GOM ranging from 0.1 pg m^{-3} over the Adriatic (Sprovieri and Pirrone, 2008) to 4018 pg m^{-3} over the Dead Sea (Obrist et al., 2011) (Tables S2 and S3; references therein). Frequency distributions of 24 h average GOM and PBM concentrations from a site situated in the Mediterranean MBL exhibited log-normal distributions with the maximum frequency at around 59 and 48 pg m^{-3}, respectively (Pirrone et al., 2003). One of the major findings from Sprovieri et al. (2003) was constant presence of GOM averaged at 7.9 ± 0.8 pg m^{-3} in the MBL over a 6000 km long cruise path around the Mediterranean Sea. In a 1 year dataset from 2008, Beldowska et al. (2012) showed 24 h PBM concentrations varied over 2–142 pg m^{-3} averaged at 20 ± 18 pg m^{-3} with 93 % on average in the coarse fraction (> 2 µm) over the southern Baltic Sea.

In springtime Arctic, the highest concentrations of GOM at 900–950 pg m^{-3} were observed during the 1998–2001 BAMS. Very high springtime PBM concentrations (mean 394 pg m^{-3}, 47–900 pg m^{-3}, 1 h) were reported over Beaufort Sea sea ice by Steffen et al. (2013). This was an order of magnitude higher than concurrent GOM concentrations (mean 30 pg m^{-3}, 3.5–104.5 pg m^{-3}) and even larger than those in temperate regions, where particle concentrations tended to be large. In comparison, Sommar et al. (2010) found very low GOM and PBM over the summertime Arctic Ocean.

Over the Antarctica, 2 h GOM concentrations ranged over 10.5–334 pg m^{-3} averaged at 116.2 ± 77.8 pg m^{-3} in Terra Nova Bay during spring–summer 2000 (Sprovieri et al., 2002), and a similar range was also observed by Temme et al. (2003b) at the Neumayer Station in summer 2001 (Table S2). A range of 30–140 pg m^{-3} (80 min) was reported for peaks of GOM in summer 2007 (Soerensen et al., 2010). Concentrations of 1 h PBM from Temme et al. (2003b) varied over 15–120 pg m^{-3}, a range a factor of 3 smaller than that of concurrent GOM, tracking GOM well only at a lower level. Different from the Arctic, summertime GOM concentrations over the Antarctic were orders of magnitude larger.

2.2.2 Hemispheric difference

Hemispheric gradient has been measured in both GOM and PBM since the early 1980s (Slemr et al., 1985; Soerensen et al., 2010). In the first shipboard study by Slemr et al. (1985), PBM concentrations of 0.013 ± 0.018 and 0.007 ± 0.004 ng m^{-3} over the North and South Atlantic Ocean, respectively, were derived from Hg concentrations in rain water. About 3 decades later Soerensen et al. (2010) reported hemispheric difference of GOM with a NH average of 0.3 ± 3 pg m^{-3} in summer and 0.8 ± 2 pg m^{-3} in spring, and a seasonally invariable SH average of 4.3 ± 0.14 pg m^{-3}.

2.2.3 Temporal variations from diurnal to long-term trend

Diurnal variation

While some studies found a lack of diurnal variation in GOM (Sheu and Mason, 2001; Aspmo et al., 2006; Temme et al., 2003b), many reported distinct diurnal variation with noon-afternoon peaks and nighttime minimums in various oceanic regions (Mason et al., 2001; Mason and Sheu, 2002; Lindberg et al., 2002; Laurier et al., 2003; Sprovieri et al., 2003, 2010; Laurier and Mason, 2007; Mao et al., 2008; Chand et al., 2008; Sigler et al., 2009b; Soerensen et al., 2010; Mao and Talbot, 2012; Wang et al., 2014). Over the Atlantic amplitude values varied from 0.27 pg m^{-3} in winter 2010 near the coast of southern New Hampshire, USA (Mao and Talbot, 2012), to > 80 pg m^{-3} on the cruise from Barbados via Bermuda to Baltimore, Maryland, USA (Mason and Sheu, 2002; Laurier and Mason, 2007). Over the Pacific amplitude values exceeded 80 pg m^{-3} (Laurier et al., 2003; Chand et al., 2008; Wang et al., 2014). Over the Mediterranean Sea and its neighboring seas, diurnal amplitude reached up to 35 pg m^{-3} (Sprovieri et al., 2003, 2010). The most pronounced diurnal variation was observed in the springtime Arctic with noontime peaks up to 900–950 pg m^{-3} and near-zero concentrations at night (Lindberg et al., 2002).

The diurnal pattern of PBM concentrations, measured using a Tekran speciation unit, at a midlatitude North Atlantic near-coastal MBL site was in general not consistent between seasons and years with seasonally averaged daily peaks 0.2–0.7 ppqv (1.7–6.2 pg m^{-3}) at varying time of a day (Mao and Talbot, 2012). The Tekran PBM instrument measures PBM on particles < 2.5 µm. Using a 10-stage impactor, Feddersen et al. (2012), perhaps the first to study the size distribution of PBM in MBL, reported PBM concentrations (up to 0.25 ppqv, i.e., 2.2 pg m^{-3}, in 3.3–4.7 µm) in 10 size fractions (< 0.4 µm to > 10 µm) at the same MBL location from Mao and Talbot (2012), and found a diurnal cycle with daily maximums at around 16:00 UTC (noon local time) and minimums around sunrise.

Seasonal to annual variation

Studies reported distinct seasonal variation in GOM with higher concentrations in warmer months and lower in colder months (Mason et al., 2001; Mason and Sheu, 2002; Pirrone et al., 2003; Laurier and Mason, 2007; Sigler et al., 2009a; Sprovieri et al., 2010; Soerensen et al., 2010; Mao and Talbot, 2012; Obrist et al., 2011; Moore et al., 2013; Wang et al., 2014; Angot et al., 2014). A fairly flat baseline with negligible annual variation in GOM was observed at a midlatitude North Atlantic MBL site near southern New

Hampshire, USA, in a 3 year dataset, with more variability in higher mixing ratios and seasonal median values ranging from 0.03 ppqv ($\sim 0.27\,pg\,m^{-3}$) in winter 2010 to 0.55 ppqv ($\sim 4.9\,pg\,m^{-3}$) in summer 2007 (Mao and Talbot, 2012). Over the Mediterranean, the fall 2004 campaign experienced no production of GOM, whereas the summer 2005 campaign saw very high concentrations varying over 21–40 $pg\,m^{-3}$ (Sprovieri et al., 2010a). In the Dead Sea MBL, AMDEs resulting in 1 h GOM up to 700 $pg\,m^{-3}$ occurred more frequently in the summer than in winter (Obrist et al., 2011; Moore et al., 2013).

In the Arctic MBL, several hundreds of $pg\,m^{-3}$ GOM concentrations were observed in spring (Lindberg et al., 2002; Steffen et al., 2013) and very low GOM and PBM concentrations in summer (Sommar et al., 2010). Quite differently, summertime GOM concentrations over the Antarctic seemed to be orders of magnitude larger (Sprovieri et al., 2002; Temme et al., 2003b; Soerensen et al., 2010).

Some studies observed seasonal variation in PBM. Sprovieri et al. (2010a) found PBM concentrations on average were more than a factor of 2 higher during high-Hg episodes in the fall than during the summertime ones over the Mediterranean Sea. Beldowska et al. (2012) measured an average 24 h PBM of 15 $pg\,m^{-3}$ and a 3–67 $pg\,m^{-3}$ range in the non-heating season compared to an average of 24 $pg\,m^{-3}$ and a range of 2–142 $pg\,m^{-3}$ in the heating season. The PBM measurements at a North Atlantic coastal site using a 10-stage impactor showed distinct seasonal variation with 50–60 % of PBM in coarse fractions, 1.1–5.8 µm, composed largely of sea salt aerosols at both sites in summer and 65 % in fine fractions in winter (Feddersen et al., 2012). Over the Indian Ocean significantly higher concentrations were observed in winter than in summer ($2.18 \pm 1.56\,ng\,m^{-3}$ vs. $1.79 \pm 1.15\,pg\,m^{-3}$) (Angot et al., 2014).

2.2.4 Mechanisms driving the observed temporal variabilities

Factors causing episodic high and low concentrations

Long-range transport of air masses of terrestrial origin with high-PBM concentrations was evidenced in elevated crustal enrichment factors in the PBM samples (Lamborg et al., 1999). An episode of high-GOM concentrations coincided with a passing hurricane was linked to downward mixing of air aloft with higher GOM (Prestbo, 1997; Mason and Sheu, 2002). Low-GOM concentrations were found to be concurrent with high humidity (e.g., fog) and rainfall but the highest concentrations on the day after such events if temperatures were elevated (Mason and Sheu, 2002). High nighttime concentrations of GOM in the Mediterranean Basin were observed in anthropogenic plumes identified using backward trajectories (Sprovieri et al., 2010a). The GOM concentrations in air masses of marine origin at a site on the East Pacific coast were unusually high ranging over 200–700 $pg\,m^{-3}$ (Timonen et al., 2013). The high-GOM concentrations were thought to be partitioned back from the PBM that was accumulated on aqueous super-micron sea salt aerosols in the MBL when being lofted above the MBL, and an anticorrelation between GOM and GEM was found in air masses of marine origin indicating strong in situ oxidation of GEM.

Diurnal variation

The lack of GOM diurnal variation was speculated to result from diverse air masses with different concentrations converging at the location leading to the removal of diurnal variation in GOM (Sheu and Mason, 2001), and from low solar radiation ($< 200\,W\,m^{-2}$) at higher latitudes (Aspmo et al., 2006). The majority of the studies reporting significant diurnal variation in GOM attributed it to photooxidation, loss via dry deposition, and oceanic evasion, which was backed up by modeling studies (Hedgecock et al., 2003, 2005; Laurier et al., 2003; Selin et al., 2007; Strode et al., 2007).

It was generally found that GOM concentrations were positively correlated with solar radiation flux and anticorrelated with relative humidity and at times with O_3 (Mason and Sheu, 2002; Laurier and Mason, 2007; Soerensen et al., 2010; Mao et al., 2012). The correlation between GOM and UV radiation flux indicated photochemical processes, and the anticorrelation between GOM and O_3 was caused by processes destroying O_3 and producing GOM (Mason and Sheu, 2002; Laurier and Mason, 2007), especially the oxidation reactions in the presence of deliquescent sea salt aerosols (Sheu and Mason, 2004). The fact that GOM daytime peaks over the Pacific increased with lower wind speeds and stronger UV radiation suggested that GOM was produced in situ via photochemically driven oxidation (Laurier et al., 2003; Chand et al., 2008). Chand et al. (2008) estimated the magnitude of GOM close to the amount produced from the reaction of GEM + OH alone. Mao and Talbot (2012) suspected that unknown production mechanism(s) of GOM in the nighttime MBL kept the levels above the LOD. Positive correlation between GOM/PBM and temperature indicated possible temperature dependence of certain oxidation reactions and gas-particle partitioning, whereas the anticorrelation between GOM/PBM and wind speed indicated enhanced loss via deposition caused by faster wind speed over water (Mao et al., 2012).

No consistent diurnal variation in PBM measured using a Tekran speciation unit suggested more complicated processes than photochemistry involved in PBM budgets (Mao et al., 2012). However, Feddersen et al. (2012) found diurnal variation in 10-stage impactor PBM measurement data and speculated that GEM oxidation drove the PBM daytime maximum at around 16:00 UTC (noon local time) and depositional loss at night without replenishment led to the minimum around sunrise. In the same study, the large peaks of PBM appeared to be of continental origin.

Seasonal to annual variation

Larger concentrations of GOM in spring and/or summer were generally associated with stronger photo oxidation, biological activity, biomass burning, oceanic, and anthropogenic emissions, whereas low concentrations with wet deposition (Lindberg et al., 2002; Mason and Sheu, 2002; Temme et al., 2003b; Pirrone et al., 2003; Sprovieri et al., 2003; Hedgecock et al., 2004; Laurier and Mason, 2007; Sprovieri and Pirrone, 2008; Sprovieri et al., 2010; Soerensen et al., 2010; Obrist et al., 2011; Mao et al., 2012; Angot et al., 2014; Wang et al., 2014). The positive correlation between GOM concentration and solar radiation was used to explain warm season maximums of GOM based on the same line of reasoning that was used to explain daytime peaks of GOM (Mason and Sheu, 2002; Pirrone et al., 2003; Mao et al., 2012). Observed seasonal variation in PBM was attributed to anthropogenic influence and gas-particle partitioning as well as condensation and coagulation of fine particles (Sprovieri et al., 2010a; Beldowska et al., 2012).

Over the Mediterranean Sea and its neighboring seas, it was generally thought that meteorological conditions combined with anthropogenic, oceanic, and biomass emissions caused GOM and PBM seasonal variation (e. g. Pirrone et al., 2003; Sprovieri et al., 2003; Hedgecock et al., 2004; Sprovieri and Pirrone, 2008). A case in point is the seasonal contrast of no production and little variation in GOM due likely to strong removal under the wet conditions in fall 2004 and very high concentrations due to strong oxidation under dry, sunny conditions in summer 2005 (Sprovieri et al., 2010). Sensitivity box model simulations suggested that the Hg + Br controlled the production rate of GOM without contributions from the oxidation reactions by O_3 and OH and that HgBr was quickly converted to GOM. In the same study it was brought to attention that biomass burning and ship emissions in the region were not included in the emission inventory but could be important to ambient concentrations (Sprovieri et al., 2010). The authors suggested that ship emissions could become a more important source of contaminants as emissions from other sources were being more stringently controlled, and also the Mediterranean was a place where busy shipping routes ran close to population centers. However, no studies have demonstrated that ship emissions were an important source of Hg.

In the Dead Sea MBL, frequent occurrences of MDEs in the summer were linked to higher BrO concentrations indicative of Br-initiated oxidation of GEM despite high temperature and sometimes low-BrO concentrations (Obrist et al., 2011). There is apparent discrepancy between our theoretical understanding of the conditions required for Br-initiated GEM oxidation and the real atmospheric conditions in the summertime Dead Sea MBL.

Wang et al. (2014) proposed iodine in a two-step mercury oxidation mechanism, where BrHgI was hypothetically formed, helped to reconcile the modeled GOM with the observed annual maximum GOM in October over the equatorial Pacific. The authors mentioned that HO_2 and/or NO_2 aggregation with HgBr from Dibble et al. (2012) could be another possibility and further suggested that a major process in representing Hg oxidation is missing in current models.

Lindberg et al. (2002) found that springtime Arctic maximum concentrations of GOM at 900–950 $\mathrm{pg\,m^{-3}}$ corresponded to open leads over sea ice and an extensive area of elevated BrO concentrations under the calmest conditions and strongest UV radiation. Low GOM and unusually large PBM concentrations over Beaufort Sea sea ice in spring 2009 were speculated to be caused by low temperatures and GOM formation followed by adsorption onto available sea salt and sulfate aerosols, as well as ice crystals around the sea ice (Steffen et al., 2013). In contrast, very low summertime Arctic GOM and PBM were due possibly to low in situ oxidation of GEM and enhanced physical scavenging as a result of low visibility and high relative humidity (Sommar et al., 2010).

Higher concentrations of GOM over the Antarctic Ocean were first proposed by Sprovieri et al. (2002) to be produced from gas-phase oxidation of GEM by O_3, H_2O_2, and OH together with favorable physical conditions such as PBL height. Temme et al. (2003b) found that the highest concentrations of GOM corresponding to the lowest concentration of GEM falling below the LOD (1.1 $\mathrm{pg\,m^{-3}}$) during MDEs in summer were associated with the air masses having a maximum contact with sea ice (coverage > 40 %) over the South Atlantic Ocean, which was speculated to contain abundant reactive Br, released from sea salt associated with sea ice. Summertime GOM was found to be correlated with GEM due probably to in situ oxidation and buildup (Soerensen et al., 2010) and was also observed to be anticorrelated with GEM due solely to oxidation (Temme et al., 2003b; Sprovieri et al., 2002).

3 Continental boundary layer

In this section, continental sites are defined as inland sites located in non-polar regions and exclude locations impacted by the MBL, e.g., coastal sites and oceans.

3.1 TGM/GEM

3.1.1 Concentration metrics

Field measurements of TGM/GEM at continental sites were conducted mainly in Asia, Canada, Europe, and USA. Very few TGM/GEM measurements have been made at inland sites in the SH. Of all the four regions, the median concentrations of TGM or GEM were 1.6 $\mathrm{ng\,m^{-3}}$ at remote and rural surface (low elevation) sites, 2.1 $\mathrm{ng\,m^{-3}}$ at urban surface sites, and 1.7 $\mathrm{ng\,m^{-3}}$ at high-elevation sites (Fig. 2a). TGM/GEM ranged over 0.1–11.3 $\mathrm{ng\,m^{-3}}$ at remote sites, 0.2–18.7 $\mathrm{ng\,m^{-3}}$ at rural sites, 0.2–702 $\mathrm{ng\,m^{-3}}$ at urban sites, and 0.6–106 $\mathrm{ng\,m^{-3}}$ at high-elevation sites. Overall these

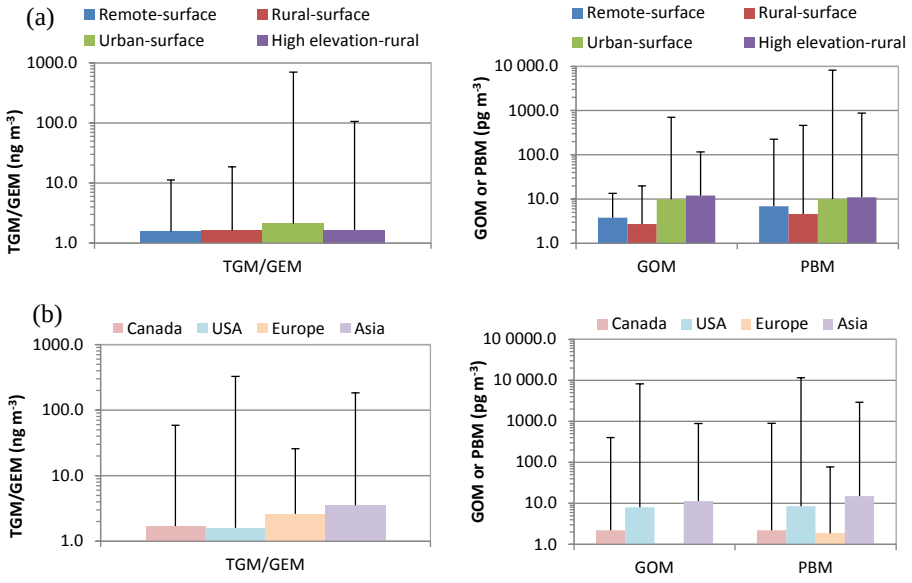

Figure 2. Median and range in TGM/GEM, GOM and PBM by site category **(a)** and by geographical region **(b)**. Bar graph represents the median and error bar represents the maximum, estimated from the values in the literature as shown in Tables S4–S6.

statistics indicate that TGM/GEM at continental urban sites were higher and had larger variability than rural and remote surface sites and high-elevation sites in the NH. By geographical region (Fig. 2b), the median TGM/GEM in Asia, comprising of sites predominantly in China and a few sites in Korea and Japan, were higher by 26–55 % than those in Europe, Canada, and USA in this respective order. Although a higher median TGM/GEM was found in Asia, the maximum single 5 min concentration was recorded in the USA (324 ng m^{-3}, Engle et al., 2010). The 5 min maximum TGM/GEM among the four regions was the lowest in Europe (23 ng m^{-3}; Witt et al., 2010b). It is important to note that most urban sites in the literature are located in North America and Europe, and hence the higher TGM/GEM at continental urban sites as shown in Fig. 2b were predominantly driven by measurements at those sites (instead of Asian sites). A summary of the mean and the range of TGM/GEM as well as the distribution of mean TGM/GEM at individual continental sites can be found in Fig. S1 and Table S4. Statistics from studies prior to 2009 are referred to in Sprovieri et al. (2010b).

3.1.2 Temporal variations from diurnal cycle to long-term trends

Diurnal variation

At remote surface locations, the diurnal variation of TGM/GEM is characterized by a daytime increase reaching a maximum concentration in the afternoon and nighttime decrease (Manolopoulos et al., 2007; Cheng et al., 2012). At rural surface and high-elevation sites, several different diurnal patterns have been reported. The first pattern, similar to remote surface locations, is an early morning minimum, followed by midday to afternoon maximum and decrease at night (Swartzendruber et al., 2006; Yatavelli et al., 2006; Choi et al., 2008, 2013; Fu et al., 2008, 2009, 2010a, 2012b; Lyman and Gustin, 2008; Mao et al., 2008; Obrist et al., 2008; Faïn et al., 2009; Sigler et al., 2009; Mazur et al., 2009; Nair et al., 2012; Mao and Talbot, 2012; Eckley et al., 2013; Parsons et al., 2013; Cole et al., 2014; Brown et al., 2015; Zhang et al., 2015). The second diurnal pattern typically observed is a higher nighttime TGM/GEM than daytime. This tends to occur in Asia and more polluted sites outside of Asia, e.g., abandoned Hg mines and cement plants (Lyman and Gustin, 2008; Wan et al., 2009a; Rothenberg et al., 2010; Li et al., 2011; Nguyen et al., 2011; Fu et al., 2012a; Gratz et al., 2013; Zhang et al., 2013; Cole et al., 2014). The third pattern found at rural surface and elevated sites is a weak or lack of diurnal pattern in TGM/GEM (Choi et al., 2008, 2013; Mao et al., 2008; Sigler et al., 2009; Engle et al., 2010; Rothenberg et al., 2010; Mao and Talbot, 2012; Zhang et al., 2013; Han et al., 2014).

At urban surface sites, the predominant diurnal pattern is an increase in TGM/GEM throughout the night that leads to a maximum in the early morning and a decrease in TGM/GEM in the afternoon (Stamenkovic et al., 2007; Li et al., 2008; Choi et al., 2009; Lyman and Gustin, 2009; Song et al., 2009; Liu et al., 2010; Witt et al., 2010b; Nguyen et al., 2011; Nair et al., 2012; Zhu et al., 2012; Gratz et al., 2013; Kim et al., 2013; Civerolo et al., 2014; Cole et al., 2014; Han et al., 2014; Lan et al., 2012, 2014; Xu et al., 2014, 2015). The diurnal amplitude tends to be higher during summer compared to other seasons (Stamenkovic et al., 2007; Peterson et al.,

Table 1. Summary of predominant temporal patterns of speciated atmospheric mercury at continental sites in the Northern Hemisphere.

	Diurnal variation	Seasonal variation
TGM/GEM		
Rural	Daytime maximum, nighttime minimum	Winter–spring maximum and summer–fall minimum
Urban	Nighttime maximum, daytime minimum	No predominant pattern
High elevation	Daytime maximum, nighttime minimum	Winter–spring maximum and summer–fall minimum
GOM		
Rural	Midday to late afternoon maximum, nighttime minimum * Exception: nighttime maximum at urban and elevated sites	No predominant pattern
Urban		Spring or summer maximum
High elevation		No predominant pattern
PBM		
Rural	No predominant pattern	Maximum during heating season
Urban	No predominant pattern	Maximum during heating season * Exception: summer maximum
High elevation	No predominant pattern	Maximum during heating season

2009; Civerolo et al., 2014; Lan et al., 2012, 2014; Xu et al., 2014). Diurnal variations with daytime maximum and early morning minimum have also been observed at urban surface sites (Fostier and Michelazzo, 2006; Rothenberg et al., 2010; Witt et al., 2010b; Jiang et al., 2013; Han et al., 2014).

Seasonal variation

The seasonal variation in TGM/GEM at some continental remote surface sites can be characterized by a winter to early-spring maximum and lower summer/fall concentrations (Manolopoulos et al., 2007; Cheng et al., 2012). At other remote sites, a completely opposite seasonal pattern was found with higher summer/fall concentrations than winter/spring (Abbott et al., 2008; Cole et al., 2014). The predominant seasonal TGM/GEM trend at rural surface and elevated sites is the winter to spring maximum and summer/fall minimum (Zielonka et al., 2005; Yatavelli et al., 2006; Choi et al., 2008; Fu et al., 2008, 2009, 2010a; Mao et al., 2008; Sigler et al., 2009a; Mazur et al., 2009; Engle et al., 2010; Mao and Talbot, 2012; Nair et al., 2012; Chen et al., 2013; Parson et al., 2013; Cole et al., 2014; Marumoto et al., 2015). Other studies conducted in rural sites and elevated sites found higher TGM/GEM during warm seasons (spring/summer) than in the winter (Weiss-Penzias et al., 2007; Obrist et al., 2008; Nguyen et al., 2011; Eckley et al., 2013; Zhang et al., 2013, 2015).

The seasonal patterns at continental urban surface sites can be vastly different from each other. Five major seasonal patterns have been identified including (1) a winter to spring maximum (Fostier and Michelazzo, 2006; Stamenkovich et al., 2007; Choi et al., 2009; Peterson et al., 2009; Civerolo et al., 2014; Xu et al., 2015), (2) a summer TGM/GEM maximum (Xu and Akhtar, 2010; Jiang et al., 2013), (3) higher TGM during both winter and summer (Xu et al., 2014), (4) higher TGM/GEM during spring/summer (Liu et al., 2007, 2010; Song et al., 2009; Nair et al., 2012; Zhu et al., 2012; Hall et al., 2014), and (5) an absence of a clear seasonal trend (Kim et al., 2013; Civerolo et al., 2014; Marumoto et al., 2015). Table 1 summarizes the predominant diurnal and seasonal patterns observed at rural, urban, and high-elevation continental sites.

Long-term trends

At rural sites across Canada, TGM decreased at a rate of 0.9–3.3 % per year between 1995 and 2011, which was determined using 5–15 years of TGM data depending on the location (Cole et al., 2014). A GEM decrease of $0.056\,\mathrm{ng\,m^{-3}\,yr^{-1}}$ from 2005 to 2010 was found at an elevated site in New Hampshire (Mao and Talbot, 2012). Widespread declines in GEM across North America between 1997 and 2007 have also been reported (Weiss-Penzias et al., 2016); however, the trends were not determined sepa-

rately for rural and urban sites. No significant trends in TGM were found at urban/industrial sites in the UK from 2003–2013 (Brown et al., 2015) and at another urban site in Seoul, Korea, from 2004 to 2011 (Kim et al., 2013). However, a short-term annual TGM decrease from 2.0 to 1.7 ng m^{-3} was recorded at an urban site in Windsor, Canada, from 2007 to 2009 (Xu et al., 2014). At a chlor-alkali site in the UK, TGM declined by 1.36 ± 0.43 ng m^{-3} yr^{-1} from 2003 to 2012 (Brown et al., 2015). Weigelt et al. (2015) determined annual TGM trends for different air masses arriving at Mace Head, Ireland, between 1996 and 2013. Specifically for continental airflows, TGM decreased by 0.0240 ± 0.0025 ng m^{-3} yr^{-1} for polluted air masses from Europe, which was a slightly faster decline compared to marine airflows from the North Atlantic Ocean (-0.0209 ± 0.0019 ng m^{-3} yr^{-1}) and the SH (-0.0161 ± 0.0020 ng m^{-3} yr^{-1}). In certain months, the TGM decreases associated with local and European airflows (0.047–0.051 ng m^{-3} yr^{-1}) were greater than other months (Weigelt et al., 2015).

3.1.3 Mechanisms driving the observed temporal variabilities

Diurnal variation of TGM/GEM

TGM/GEM was higher during daytime than nighttime and often declined to a minimum in the early morning at remote, rural, high elevation, and some urban surface sites (Table 1). One of the mechanisms driving this diurnal pattern involved meteorological parameters, such as temperature, the increase of which enhances TGM/GEM volatilization (Manolopoulos et al., 2007; Mao et al., 2012; Jiang et al., 2013; Han et al., 2014). Surface emissions of TGM can occur during daytime from soil and snow as temperature and solar radiation increases (Mao et al., 2012; Cole et al., 2014). Solar radiation minimizes the activation energy required for Hg emissions (Zhu et al., 2012) and increases Hg photoreduction in soil and snow (Steffen et al., 2008; Zhu et al., 2012; Hall et al., 2014; Xu et al., 2014, 2015). This process appeared to be especially relevant at sites with elevated Hg in soil (Lyman and Gustin, 2008; Brown et al., 2015) because of a larger flux gradient. Dry deposition of GEM in the night might have also played a role since deposition was typically observed in nighttime in contrast to emission during daytime (Zhang et al., 2009). Fog or dew formation occurring in the late summer was believed to have caused GEM depletion in the early morning hours by capturing GEM in fog or dew water (Manolopoulos et al., 2007; Mao and Talbot, 2012). Another driving mechanism of this TGM/GEM diurnal pattern was the change in the boundary layer mixing height. Lower TGM/GEM during nighttime is due to TGM/GEM deposition as the nocturnal inversion layer forms. In the morning, the nocturnal inversion breaks down and mixes with TGM/GEM-rich air in the residual layer and subsequently leads to increasing TGM/GEM during the day (Yatavelli et al., 2006; Mao et al., 2008; Mazur et al., 2009; Mao and Talbot, 2012; Nair et al., 2012; Choi et al., 2008, 2013; Jiang et al., 2013; Cole et al., 2014). At elevated sites, there was a transition from the sampling of boundary layer during daytime to free troposphere air at night, which was driven by mountain–valley atmospheric patterns (Obrist et al., 2008). During daytime, mountain breeze causes moist air to ascended from the surface to higher altitudes carrying with it GEM from the boundary layer (Swartzendruber et al., 2006; Obrist et al., 2008; Fu et al., 2010a, 2012b; Zhang et al., 2015). At night, drier free tropospheric air impacted the elevated site leading to lower GEM and water vapor and higher GOM and ozone (Obrist et al., 2008). A lack of diurnal variability was also reported at some rural surface locations, although the driving mechanism is not quite clear. At an elevated site, the sampling of air above the nocturnal boundary layer and lack of anthropogenic sources or GEM oxidants near the site led to constant GEM during most of the time except in the summer (Mao et al., 2008; Sigler et al., 2009a; Mao and Talbot, 2012). Thus, this differed from other mountain sites, which were affected by surface emissions and local/regional transport of GEM from the boundary layer during daytime.

At most urban sites and some elevated and polluted rural sites, the nighttime TGM concentrations were higher than daytime, and the maximum concentration typically occurred in the early morning before sunrise (Table 1). This type of diurnal variation was driven by nighttime accumulation of TGM/GEM near the surface due to a shallow nocturnal boundary layer and dilution during the day initiated by convective mixing with cleaner air aloft as the mixing layer increases (Stamenkovic et al., 2007; Li et al., 2008; Lyman and Gustin, 2008, 2009; Choi et al., 2009; Wan et al., 2009a; Rothenberg et al., 2010; Witt et al., 2010b; Li et al., 2011; Nguyen et al., 2011; Fu et al., 2012a; Nair et al., 2012; Zhu et al., 2012; Gratz et al., 2013; Kim et al., 2013; Zhang et al., 2013; Cole et al., 2014; Lan et al., 2012, 2014; Xu et al., 2014). The shallow nocturnal boundary layer was often associated with high TGM coinciding with low wind speeds at night (Li et al., 2008; Fu et al., 2012a; Lan et al., 2014). Increases in nighttime concentrations could also be driven by nighttime sources, such as emissions from mercury mining regions (Lyman and Gustin, 2008) and local emissions occurring at night (Song et al., 2009; Wan et al., 2009a; Rothenberg et al., 2010; Gratz et al., 2013; Kim et al., 2013). At urban surface sites, studies suggested the driving mechanisms for the morning maximum were surface emissions (Zhu et al., 2012; Hall et al., 2014; Xu et al., 2014, 2015), volatilization of Hg from dew (Zhu et al., 2012), and vehicular traffic emissions evident by correlations between TGM/GEM and CO and NO_x (Zhu et al., 2012; Xu et al., 2015). However, there is little research suggesting significant amounts of Hg from vehicular emissions (Conaway et al., 2005; Landis et al., 2007; Won et al., 2007). The general view is that the global contribution from petroleum fuel combustion represented 0.00013 % of the total anthropogenic emissions and

thus can be neglected in global assessment of Hg emissions (Pirrone et al., 2010). The lower TGM/GEM observed in the afternoon was driven by GEM oxidation (Stamenkovic et al., 2007; Choi et al., 2009; Lyman and Gustin, 2009; Li et al., 2011; Nguyen et al., 2011; Kim et al., 2013; Zhang et al., 2013; Xu et al., 2014, 2015).

Many studies conducted in urban areas found a larger diurnal amplitude during summer than other seasons. The major driving mechanism for this larger amplitude originated from higher solar radiation and temperature, which increased the boundary layer mixing height in the summer (Civerolo et al., 2014; Xu et al., 2014). Higher solar radiation during summer also increased photochemical reactions, like GEM oxidation. The larger diurnal variation was also attributed to increases in uptake and re-emissions by vegetation and power plant emissions from air conditioner use during summer nights (Xu et al., 2014). The shift in the timing of the TGM/GEM maximum varied with season at some urban sites. During spring in Windsor, Canada, the decrease in TGM earlier in the afternoon was thought to be due to increase photochemical processes resulting from higher solar radiation and lower GEM emissions due to less vegetation coverage in the spring (Xu et al., 2014). In Nanjing, China, the peak concentration occurring later in the morning during spring was driven by prolonged sunlight hours (Zhu et al., 2012).

Site characteristics may have different impacts on the diurnal variation. During nighttime, GEM at an urban site was significantly higher than a rural site suggesting higher GEM fluxes from buildings and pavement than vegetation and soil (Liu et al., 2010), but may be simply caused by stronger and more anthropogenic sources in urban areas. The diurnal amplitude at an urban site was greater than a suburban site in one study; however, the reason was not known (Civerolo et al., 2014). In the same study, nighttime GEM was 25–30 % higher than daytime for the urban site close to the Atlantic Ocean, whereas the GEM difference between night and day was only 10 % at an inland suburban site (Civerolo et al., 2014). The study suggested that the higher halogen concentrations in marine environments increased GEM oxidation and subsequently, the loss of GEM in the afternoon leading to larger diurnal variation. At a different coastal-urban location, nighttime GEM was only slightly higher than daytime because of the cleaner air transported from the marine environment (Nguyen et al., 2011). These studies suggested that MBL influence could lead to very different diurnal patterns. Sites continuously impacted by Hg point sources likely contributed to the large short-term fluctuations in the diurnal patterns at some urban sites (Rutter et al., 2008; Engle et al., 2010; Witt et al., 2010b).

Seasonal variation of TGM/GEM

The seasonal variation exhibiting a winter to spring maximum in remote, rural, urban and high-elevation environments (Table 1) was suggested to be driven by multiple mechanisms, including anthropogenic emissions for winter heating (coal and wood combustion), reduced atmospheric mixing, decreased GEM oxidation, less scavenging, and emissions from soil, vegetation, and melting snow in the spring (Stamenkovic et al., 2007; Choi et al., 2008; Mao et al., 2008; Sigler et al., 2009a; Peterson et al., 2009; Wan et al., 2009a; Cheng et al., 2012; Mao and Talbot, 2012; Civerolo et al., 2014; Cole et al., 2014; Xu et al., 2015). The lower TGM/GEM during summer has been attributed to increased GEM oxidation, uptake by vegetation, and higher wet deposition of GOM (Yatavelli et al., 2006; Fu et al., 2008, 2009; Engle et al., 2010; Xu et al., 2015). While these were the predominant driving mechanisms of the seasonal variations in the NH, the seasonal patterns could also be influenced by changes in the prevailing wind patterns (Fostier and Michelazzo, 2006; Fu et al., 2010a, 2015; Sheu et al., 2010; Chen et al., 2013; Zhang et al., 2013; Hall et al., 2014). The impact of combustion emissions from winter heating was ruled out at a subtropical site in the Pearl River Delta region of China; instead, the elevated TGM in the spring was attributed to monsoons, which advected southerly marine air masses during summer and northeasterly winds from Siberia during winter. The transition from cold dry air to warm moist air often led to strong temperature inversion and haze in the spring, which in turn inhibits pollutant dispersion. Summer and spring maxima in TGM/GEM have also been found at remote, rural, and urban atmospheres. This pattern was predominantly driven by meteorology. Higher solar radiation and temperature during summer increased GEM emissions from Hg contaminated soil (Zhu et al., 2012; Eckley et al., 2013), from vegetation at a forested agricultural site (Nguyen et al., 2011), and from urban surfaces such as soil and pavement in Windsor, Canada (Xu and Akhtar, 2010).

Long-term trends of TGM/GEM

Long-term trends of TGM/GEM over continental regions indicated a declining trend at some sites and no significant trend at others, particularly at urban sites. Previous studies partly attributed the long-term TGM trends to anthropogenic Hg emissions reductions. There has been a 60–70 % decrease in anthropogenic Hg emissions from USA and Canada; however, only up to 15 % of those emissions reductions impacted TGM at Canadian sites (Cole et al., 2014). The more rapid decline in TGM measured at Mace Head, Ireland, for local and European air masses compared to marine air masses was thought to be driven by Hg emissions reductions in Europe (Weigelt et al., 2015). The baseline TGM at Mace Head decreased at a larger rate in November than other months suggesting that it is related to lower Hg emissions from residential heating in Europe. The 21 % decline in TGM from 2006 to 2012 in urban/industrial areas of the UK was also consistent with the $0.21\,\mathrm{Mg\,yr^{-1}}$ (24 %) reduction in Hg emissions from the UK, even though the TGM trend from the 2003 to 2013 period was not statistically significant (Brown

et al., 2015). In Seoul, Korea, no significant trend in TGM was found from 2004 to 2011, consistent with the slight decrease (1 %) in coal consumption in Seoul over the same time frame (Kim et al., 2013). While TGM/GEM trends appear to be aligned with local/regional Hg emission trends, a discrepancy exists when the trend was compared to the increasing global anthropogenic Hg emissions (Sprovieri et al., 2010b; Ebinghaus et al., 2011; Cole et al., 2014). Alternative reasons for the decline in TGM could be due to faster cycling of Hg as O_3 and other oxidants have been increasing or lower emissions of previously deposited Hg (Sprovieri et al., 2010b; Ebinghaus et al., 2011). Modeling studies indicated global Hg emissions inventory have not accounted for the changes in Hg speciation emission profiles from coal combustion and reduced emissions from products containing Hg (Zhang et al., 2016).

3.2 GOM and PBM

3.2.1 Concentration metrics

The highest median GOM and PBM were found at high-elevation sites, while the lowest concentrations were found at rural surface sites. The median GOM from all locations were 12.1 pg m^{-3} at elevated sites, 9.9 pg m^{-3} at urban sites, 3.8 pg m^{-3} at remote sites, and 2.8 pg m^{-3} at rural sites (Fig. 2a), and correspondingly the median PBM concentration was 11.0, 10.0, 6.9, and 4.6 pg m^{-3}. The variabilities in GOM and PBM were greatest at urban locations; 2–3 h GOM concentrations ranged from < LOD-880 pg m^{-3} at elevated sites, < LOD-8160 pg m^{-3} at urban sites, < LOD-224 pg m^{-3} at remote sites, and < LOD-462 pg m^{-3} at rural sites (see individual site statistics and the map of mean concentrations at all sites in Fig. S1 and Table S5). Moreover, 2–3 hour PBM concentrations ranged from < LOD-1001 pg m^{-3} at elevated sites, < LOD-11 600 pg m^{-3} at urban sites, < LOD-404 pg m^{-3} at remote sites, and < LOD-205 pg m^{-3} at rural sites (Table S6). By geographical region, the median GOM in Asia was a factor of 1.4–5.1 higher than those in Canada and USA (Fig. 2b). Similarly, the median PBM in Asia was 1.8–8.1 times higher than those in Canada, Europe, and USA. This was potentially because one-third of the elevated sites were in China. The GOM and PBM maxima of 8160 and 11 600 pg m^{-3}, respectively, were both observed at an urban site in Illinois, USA (Engle et al., 2010; Tables S5 and S6).

3.2.2 Temporal variations from diurnal cycle to seasonal trends

Diurnal variation

The predominant diurnal pattern of GOM at remote, rural, urban, and elevated sites was an increase in the morning leading to a maximum sometime between midday to late afternoon and eventually decreasing at night (Yatavelli et al., 2006; Manolopoulos et al., 2007; Abbott et al., 2008; Lyman and Gustin, 2008; Faïn et al., 2009; Rothenberg et al., 2010; Cheng et al., 2012; Fu et al., 2012a; Nair et al., 2012; Eckley et al., 2013; Gratz et al., 2013; Cole et al., 2014; Civerolo et al., 2014; Marumoto et al., 2015; Zhang et al., 2015). Late evening increases in GOM were observed at some urban and elevated sites (Lynam and Keeler, 2005; Song et al., 2009; Gratz et al., 2013). The average GOM was 18–60 pg m^{-3} between midnight and early morning at two elevated sites, whereas the average daytime GOM was 9.2–39 pg m^{-3} (Swartzendruber et al., 2006; Sheu et al., 2010).

No predominant diurnal pattern was found for PBM, which was mostly measured using the Tekran speciation unit (2537-1135-1130). At rural and urban sites, the types of diurnal patterns include, daytime/afternoon peak (Yatavelli et al., 2006; Choi et al., 2008; Rothenberg et al., 2010; Cole et al., 2014), increasing during daytime leading to a nighttime peak (Nair et al., 2012; Zhang et al., 2013), or lack of variation (Cobbett and Van Heyst, 2007; Choi et al., 2008; Rothenberg et al., 2010; Cole et al., 2014).

Seasonal variation

No predominant seasonal pattern in GOM was found at remote, rural, urban, and elevated sites. At remote sites, some studies observed a winter to early-spring maximum and lower concentrations during summer/fall (Manolopoulos et al., 2007; Cheng et al., 2012), whereas higher summer/fall than winter/spring concentrations were also reported (Abbott et al., 2008). In rural and elevated sites, the maximum concentration occurred in different seasons. At urban sites, the maximum GOM typically occurred in warmer seasons, e.g., spring or summer (Song et al., 2009; Liu et al., 2010; Choi et al., 2013; Wang et al., 2013; Gratz et al., 2013; Civerolo et al., 2014; Han et al., 2014; Marumoto et al., 2015; Xu et al., 2015). Higher PBM and total particulate Hg (TPM) during colder seasons than summer was a highly ubiquitous trend for remote, rural, urban, and elevated sites (Zielonka et al., 2005; Choi et al., 2008; Wan et al., 2009b; Liu et al., 2010; Kim et al., 2012; Gratz et al., 2013; Beldowska et al., 2012; Marumoto et al., 2015; Schleicher et al., 2015; Zhang et al., 2015). However, increases in PBM also occurred during summer in a few studies (Song et al., 2009; Huang et al., 2010; Cheng et al., 2012).

3.2.3 Mechanisms driving the observed temporal variabilities

Diurnal variations of GOM and PBM

The widespread observation of a midday to late afternoon peak in GOM at continental sites (Table 1) often coincided with meteorological parameters, such as solar radiation and temperature, and/or ozone (Yatavelli et al., 2006; Abbott et al., 2008; Wan et al., 2009a; Weiss-Penzias et al., 2009; Nair et al., 2012; Mao et al., 2012; Gratz et al., 2013; Zhang et al.,

2013; Civerolo et al., 2014; Cole et al., 2014; Marumoto et al., 2015). At high-elevation sites, GOM was also inversely correlated with relative humidity, water vapor, or dew point temperature (Swartzendruber et al., 2006; Lyman and Gustin, 2008, 2009; Weiss-Penzias et al., 2009), and in some cases GOM was not correlated with O_3 (Lyman and Gustin, 2009; Peterson et al., 2009; Xu et al., 2015). These diurnal trends indicated daytime in situ photochemical production of GOM or entrainment of GOM from the free troposphere due to convective mixing. Increases in GOM during daytime at a rural site was attributed to local transport from urban areas as indicated by similarities in diurnal patterns between GOM, SO_2, and O_3 and a delay in the timing of the GOM maximum likely resulting from emissions transport (Rothenberg et al., 2010). Short-term fluctuations in the diurnal pattern of GOM also suggested the influence of point sources (Rutter et al., 2008; Engle et al., 2010). Dry deposition and scavenging of GOM by dew played a role in decreasing GOM during nighttime (Liu et al., 2007; Wan et al., 2009b; Weiss-Penzias et al., 2009; Nair et al., 2012; Choi et al., 2013; Civerolo et al., 2014). The stronger diurnal amplitude during the spring/summer coincided with stronger correlations between GOM, solar radiation, temperature, and O_3 (Yatavelli et al., 2006; Mao et al., 2012; Gratz et al., 2013; Zhang et al., 2013), which suggested that increased photochemical processes led to higher GOM. Large diurnal variation during summer was also potentially driven by high pressure, drier, and cloud-free conditions that are conducive to the buildup of GOM in the free troposphere (Lyman and Gustin, 2009).

Nighttime increases in GOM seen exclusively at urban and elevated sites (Table 1) appeared to be driven by anthropogenic emissions and the free troposphere. Nocturnal emissions and local/regional transport within the boundary layer (Lynam and Keeler, 2005; Song et al., 2009) and reduced vertical mixing in the stable nocturnal boundary layer led to higher GOM at night in urban areas (Gratz et al., 2013). At high-elevation sites, katabatic winds entrained GOM from the free troposphere. In one study, GOM from the free troposphere was believed to originate from in situ photochemical processes due to a strong inverse GEM-GOM correlation and a GOM/GEM slope near unity during an elevated GOM episode (Swartzendruber et al., 2006). While an anticorrelation between GEM and GOM was also found at another elevated site, Sheu et al. (2010) did not observe a complete photochemical conversion of GEM to GOM. The difference between these two elevated sites suggested different sources of GOM in the free troposphere. Timonen et al. (2013) found that in one type of free troposphere air mass, GEM oxidation occurred in anthropogenic plumes transported from Asia to Mt. Bachelor Observatory, USA, and converted 20 % of the GEM to GOM. A second type of air mass traveling over the Pacific Ocean resulted in 100 % GEM conversion to GOM likely because of GEM oxidation by bromine.

The driving mechanisms behind the diurnal pattern of PBM were better explored for urban sites than other site categories. Frequent spikes in hourly concentrations during daytime were attributed to point sources (Rutter et al., 2008; Civerolo et al., 2014). At a valley urban site, higher PBM and GEM during daytime suggested similar emission sources from Hg enriched areas (Lyman and Gustin, 2009). Higher PBM during daytime in the summer could also be initiated by photochemical production of GOM followed by absorption on secondary organic aerosols (Choi et al., 2013). Diurnal patterns exhibiting nighttime increases in PBM in urban areas could be due to multiple mechanisms and sources, such as nocturnal emissions and local/regional transport within the boundary layer (Song et al., 2009), reduced vertical mixing in the stable nocturnal boundary layer (Gratz et al., 2013; Xu et al., 2015), vehicular emissions in China (Xu et al., 2015), and nighttime street food vending in Beijing (Schleicher et al., 2015).

Seasonal variations of GOM and PBM

The seasonal variation characterized by higher GOM in the warm seasons (Table 1) was primarily driven by photochemical production due to increased solar radiation, O_3, and likely other atmospheric oxidants (Liu et al., 2010; Choi et al., 2013; Civerolo et al., 2014; Xu et al., 2015). Alternative reasons could be attributed to anthropogenic emissions leading to higher GOM in the summer at urban sites (Song et al., 2009; Gratz et al., 2013). Atmospheric mercury depletion events occurring at higher latitude continental sites led to higher GOM during spring (Cole et al., 2014). Free troposphere transport was a major driving mechanism for higher reactive Hg at three high-elevation western US sites (Weiss-Penzias et al., 2015). At elevated sites in China, the occurrence of higher GOM between fall and spring were attributed to coal and biofuel burning (Wan et al., 2009b) and changes in the prevailing winds that advected GOM from polluted regions (Fu et al., 2012a; Zhang et al., 2015). Lower GOM during summer was due to wet deposition (Wan et al., 2009b; Sheu et al., 2010).

Several mechanisms contributed to the increase in PBM or TPM during colder seasons (Table 1) including, local/regional coal combustion and wood burning emissions, lower mixing height, less oxidation, and increased gas-particle partitioning (Song et al., 2009; Xiu et al., 2009; Liu et al., 2010; Cheng et al., 2012; Fu et al., 2012a; Kim et al., 2012; Choi et al., 2013; Gratz et al., 2013; Wang et al., 2013; Civerolo et al., 2014; Cole et al., 2014; Schleicher et al., 2015; Xu et al., 2015). Oxidized Hg tended to partition to particles during colder seasons because of lower temperatures (Rutter et al., 2007), higher relative humidity (Kim et al., 2012), and reduced volatilization of gaseous Hg (Choi et al., 2013). Similar to GOM, decreases in PBM during summer at many sites in China were due to wet deposition (Wan et al., 2009b; Schleicher et al., 2015; Xu et al., 2015; Zhang et al., 2015) and a shift to cleaner marine airflows during summer (Kim et al., 2012). Higher PBM during warm seasons

may be driven by forest fire emissions (Eckley et al., 2013) and increased $PM_{2.5}$ available for GOM absorption at urban sites (Song et al., 2009; Schleicher et al., 2015).

4 Latitudinal variation

There are a few shipboard and airborne studies that surveyed latitudinal variation of TGM/GEM (Slemr et al., 1981, 1985, 1995; Slemr and Langer, 1992; Fitzgerald et al., 1984; Lamborg et al., 1999; Temme et al., 2003a; Aspmo et al., 2006; Soerensen et al., 2010). Bagnato et al. (2013) compiled a latitudinal distribution of TGM/GEM using measurement data from a number of shipboard measurement studies spanning the time period of 1980–2012 (Fig. 3) and showed a small but discernible interhemispheric gradient, with the highest concentrations ($\sim 3.5\,ng\,m^{-3}$) in NH midlatitudes and the lowest in SH latitudes ($\sim 0.9\,ng\,m^{-3}$), resulting from greater emissions of Hg in the more industrialized NH.

Tropospheric airborne measurements from INTEX-B (Talbot et al., 2007, 2008) and ARCTAS (Mao et al., 2010), spanning near the surface to 12 km altitude, suggested distinct seasonal variation in GEM concentrations and latitudinal gradient. On average there was an increase of ~ 50 ppqv ($\sim 0.5\,ng\,m^{-3}$) from lower latitudes ($\sim$ 20–30 ° N) to higher (60–90° N) latitudes in spring while negligible latitudinal variation in summer (Fig. 4). It was speculated that smaller latitudinal gradient of temperature in summer likely enhanced meridional circulation resulting in smaller latitudinal variation in GEM concentration in the troposphere.

A small gradient was measured in atmospheric GEM concentrations over the Pacific from $1.32\,ng\,m^{-3}$ in 14–20° N latitudes to $1.15\,ng\,m^{-3}$ in 1–15° S latitudes in October 2011 (Soerensen et al., 2014). Atmospheric GEM elevated in the northern part of the ITCZ was temporarily influenced by the northeastern trade wind that enhanced oceanic evasion, consistent with the largest evasion flux in that region.

5 Altitude variation

Airborne measurements of TGM, GEM, and/or GOM have been conducted since 1977 (Seiler et al., 1980) extending from near the surface to ~ 12 km altitude at several geographic locations (Table S7; references therein). More recent studies showed GEM concentrations remaining nearly constant vertically, slightly decreasing with altitude (Banic et al., 2003; Radke et al., 2007; Talbot et al., 2007, 2008; Mao et al., 2010). Seasonal variation was observed from surface to 7 km over Canada with $\sim 1.5\,ng\,m^{-3}$ in summer, $1.7\,ng\,m^{-3}$ in winter, $1.7\,ng\,m^{-3}$ >1 km altitude and $1.2\,ng\,m^{-3}$ below 1 km due to widespread MDEs over the sea ice in the springtime Arctic (Banic et al., 2003). During ARCTAS, Mao et al. (2010) found that the vertical extent of springtime Arctic MDEs varied from meters to 1 km depending on the thickness of the surface inversion layer.

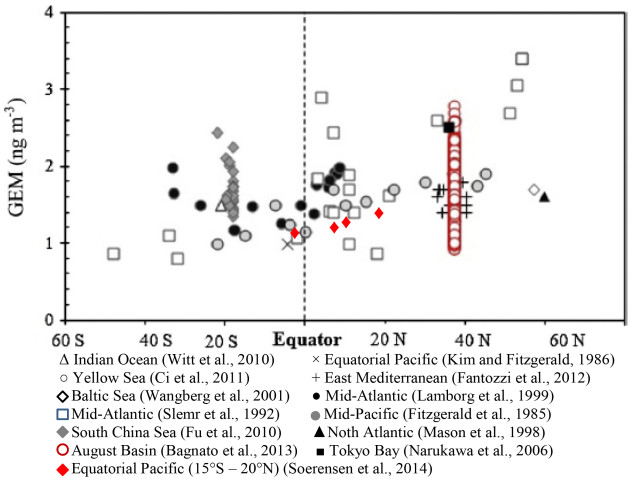

Figure 3. Compiled values for several marine/oceanic environmental systems. (Based on the figure from Bagnato et al., 2013.)

Observation of low GEM in stratospherically influenced air led to the hypothesis that the upper troposphere/lower stratosphere (UTLS) was a Hg sink region (Radke et al., 2007). With repeated measurements of depleted GEM in stratospherically influenced air coupled with enrichment of PBM in lower stratospheric aerosols (Murphy et al., 1998, 2006), Talbot et al. (2007) hypothesized that stratospheric GEM depletion was caused by fast oxidation of GEM by abundant halogen radicals and O_3 and estimated a lifetime of 2 and 0.5 days for 100 ppqv GEM oxidized by O_3 and Br, respectively. Talbot et al. (2007) suggested that stratospheric intrusion could be a source of tropospheric Hg if PBM was to be transformed back to gaseous Hg.

A $1–2\,ng\,m^{-3}$ range of upper tropospheric GEM was reported by Ebinghaus et al. (2007) and elevated GEM concentrations in biomass burning plumes from the same study suggested biomass burning representing a major mercury source. In the atmosphere of East Asia, Friedli et al. (2004) was the first to report GEM concentrations from sea level to ~ 7 km altitude under the influence of continental export from East China, showing concentrations at all altitudes higher than the global background, with the largest $6.3\,ng\,m^{-3}$ in an industrial plume mostly from coal combustion and at times from other sources including dust storms, biomass burning, and volcanic eruption. On a relevant note, Swartzendruber et al. (2008) suggested that long-range transport of Asian pollution contributed to the higher GEM concentrations above 2.5 km, which increased with altitude from $1.30 \pm 0.084\,ng\,m^{-3}$ in 0–0.5 km altitude to $1.52 \pm 0.182\,ng\,m^{-3}$ in the highest layer 5.5–6.5 km altitude over the Pacific Northwest over 13 April–16 May 2006.

Upper air GOM concentrations were first measured in spring by Lindberg et al. (2002) at 1000 and 100 m altitude immediately northeast of Point Barrow. Six aircraft surveys consistently showed that GOM concentrations de-

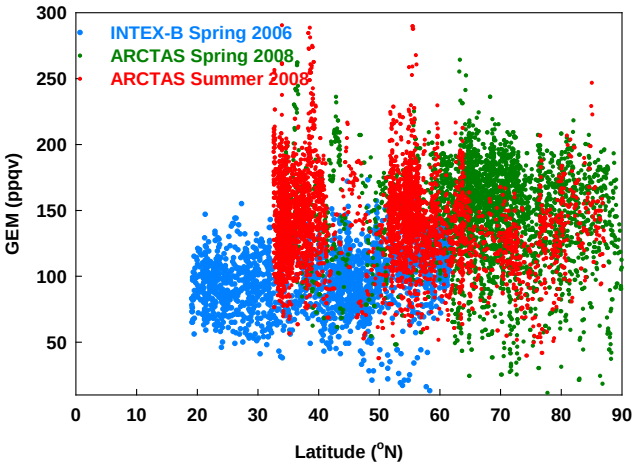

Figure 4. GEM (ppqv) from the INTEX-B in spring 2006 and ARCTAS in spring and summer 2008 (Data sources: Talbot et al., 2007, 2008; Mao et al., 2010).

creased from an average of 70 to 20 to 2 pg m^{-3} from 5 to 100 to 1000 m altitude, supporting the hypothesis that the Hg oxidation reactions occurred in the near-surface boundary layer driven by halogen compounds derived from sea-salt aerosols. In recent years, more studies attributed higher GOM concentrations in higher altitudes to lack of depositional loss, lower temperature, and/or more abundant Br radicals (Sillman et al., 2007; Lyman and Jaffe, 2011; Brooks et al., 2014; Gratz et al., 2015; Shah et al., 2016). Sillman et al. (2007) reported GOM concentrations measured in Florida increasing with height from 10 to 230 pg m^{-3}, which was reproduced using CMAQ model (Bullock and Brehme, 2002) with gas-phase oxidation reactions GEM+O_3 and GEM+OH, the latter being dominant. Lyman and Jaffe (2011) found enhanced GOM concentrations of $\sim$450 pg m^{-3} and depleted GEM in one stratospheric intrusion case and further speculated that the stratosphere was depleted in total Hg and enriched in GOM, and suggested that stratospheric intrusion could be a source of GOM to the troposphere. Near Tullahoma, TN, USA, the highest GOM concentrations (200–500 pg m^{-3}) from flights over a year were observed always at 2–4.5 km altitude with a strong seasonal variation with a wintertime minimum and a summertime maximum (Brooks et al., 2014). In the same study, limited PBM measurements exhibited similar levels to GOM at all altitudes.

In a most recent field campaign NOMADSS, the highest Hg(II) concentrations of 300–680 pg m^{-3} were observed in dry (RH < 35 %) and clean air masses during two flights over Texas at 5–7 km altitude and off the North Carolina coast at 1–3 km altitude (Gratz et al., 2015; Shah et al., 2016). Gratz et al. (2015) found, using back trajectories, that a segment of air masses with elevated GOM averaged at 0.266 ± 0.038 ng m^{-3} and ranging over 0.182–0.347 ng m^{-3} at 7 km altitude over Texas originated from the upper troposphere of the Pacific High. It was speculated that the stable, dry conditions of large-scale anticyclones resulted in a lack of GOM removal by wet deposition or in-cloud reduction and were thus ideal for GOM accumulation. They demonstrated that elevated BrOx could persist and that sufficient GOM could be produced during long-range transport in the Pacific upper troposphere. Their sensitivity analysis suggested a range of 8–13 days required to produce the observed GOM. Shah et al. (2016), using the GEOS-Chem model with tripled bromine radical concentrations or a faster oxidation rate constant for GEM+Br, increased modeled Hg(II) concentrations by a factor of 1.5–2 improving agreement with the observations, and suggested that the subtropical anticyclones were significant global sources of Hg(II).

6 Summary and recommendations

This review summarized the general characteristics in GEM, GOM, and PBM concentrations in the MBL, over land, from low to high latitudes, and from the surface to the upper troposphere, and further the factors driving such variabilities based on a great wealth of research in the literature. The Key points are summarized below.

For MBL TGM/GEM, diurnal variation in most oceanic regions featured noon to afternoon minimums due probably to in situ oxidation of GEM, while a few studies showed the opposite pattern over the Atlantic and the equatorial Pacific Ocean, attributed to enhanced oceanic evasion linked to enhanced photoreduction and biological activity. Seasonal to annual variation was generally characterized as higher (lower) concentrations in colder (warmer) months, which was largely thought to be caused by less (more) loss via oxidation in colder (warmer) months. Long-term trends have been identified at locations in Mace Head, Ireland, midlatitudinal Canada, and Cape Point, South Africa, and varied over different time periods, which was speculated to be associated with changing anthropogenic and legacy emissions, and redox chemistry.

For MBL GOM, diurnal variation was generally characterized with noon to afternoon peaks and nighttime low values and seasonal variation with higher concentrations in spring and summer and lower in fall and winter, largely attributed to GEM photooxidation as often supported by correlation of GOM with solar radiation and BrO. In one study springtime maximums were also linked to biological activity and in a few studies annual minimums were associated with scavenging by precipitation. No long-term trends have been reported for oceanic regions.

For MBL PBM, no consistent diurnal and seasonal variation has been identified in most studies, and only two studies reported seasonal variation with higher concentrations in fall/winter associated with anthropogenic emissions. One study showed no consistent diurnal variation in Tekran measurements but a clear diurnal cycle with maximums at noon

and minimums before sunrise using 10-stage impactor measurements.

For continental TGM/GEM, higher concentrations were found at urban sites than remote, rural, and elevated sites. This result is unbiased by elevated TGM/GEM from Asian sites. The predominant diurnal pattern was an early morning minimum and afternoon maximum, opposite to that at urban sites. Diurnal patterns at surface sites were thought to be driven by surface and local emissions, boundary layer dynamics, Hg photochemistry, dry deposition, and sequestering by dew. At elevated sites, mountain–valley winds appeared to be important drivers of the diurnal cycle. Seasonal variations were influenced by fossil fuel emissions for winter heating, surface emissions, and monsoons in Asia. At background sites, long-term declines in TGM were partially attributed to anthropogenic Hg emission reductions.

For continental GOM, concentrations were higher at elevated sites. However, this result may be biased by a large proportion of high-elevation studies from China where speciated atmospheric mercury are typically elevated. The predominant diurnal pattern was a noon to mid-afternoon maximum and nighttime minimum, except for nighttime increases at urban and elevated sites. The driving mechanisms of the diurnal variations were suggested to include in situ photochemical production, dry deposition, and scavenging by dew. Entrainment of GOM from the free troposphere was believed to contribute to nighttime increases at some elevated sites. No predominant seasonal pattern in GOM was found, except for higher concentrations in the spring/summer at urban sites. Photochemical production driven by strong solar radiation and atmospheric oxidants, free tropospheric transport, anthropogenic emissions, and increased wet deposition during summer appeared to affect GOM seasonal variation.

For continental PBM or TPM, no predominant diurnal pattern was found. Increases in PBM or TPM were prevalent during colder seasons and were driven by local/regional coal combustion and wood burning emissions, lower mixing height, reduced oxidation, and increased gas-particle partitioning.

TGM/GEM over the ocean surface decreased from the NH to the SH with the highest concentrations ($\sim 3.5\,\mathrm{ng\,m^{-3}}$) in NH midlatitudes and the lowest in SH ($\sim 0.9\,\mathrm{ng\,m^{-3}}$). This interhemispheric gradient was believed to suggest the majority of Hg emissions in NH, contradicting the hypothesis of large oceanic sources of Hg by previous work. However, in other studies the largest oceanic source was found in the equatorial region. Airborne measurements of TGM suggested distinct seasonal variation in latitudinal distributions, a ~ 50 ppqv ($\sim 0.5\,\mathrm{ng\,m^{-3}}$) increase in GEM concentrations from ~ 2.0–30 to 60–90° N latitudes in spring and negligible latitudinal variation in summer. It was speculated that smaller latitudinal gradient of temperature in summer likely enhanced meridional circulation resulting in smaller latitudinal variation in GEM concentration in the troposphere.

GEM concentrations remained nearly constant, slightly decreasing with altitude over the several airborne field campaign regions, and depleted GEM was found in stratospherically influenced air masses. Abundant GOM has been suggested, but only very few studies have conducted measurements of free tropospheric GOM showing concentrations of hundreds of $\mathrm{pg\,m^{-3}}$, particularly in the area of Pacific High.

Over 2 decades of extensive measurements have advanced our knowledge of the spatiotemporal variation of TGM/GEM, GOM, and PBM in numerous continental and oceanic environments. However, measurement data, especially those of PBM, remain scarce in the SH, MBL, and upper air. In oceanic regions most observations, obtained via shipboard measurements of TGM/GEM with a few exceptions as ground-based on islands, suggested composite instead of instantaneous variation. Moreover, there are hardly size-fractionated PBM measurements. The current Tekran speciation unit could only measure PBM $< 2.5\,\mu\mathrm{m}$, and Tekran PBM measurement data from a limited number of MBL and continental monitoring locations exhibited no definitive diurnal patterns in PBM concentrations. However, impactor measurements of total PBM in the MBL showed clearly defined diurnal variation with daily maximums at around noon and minimums before sunrise. These existing problems impede our gaining full knowledge of global distributions and temporal variations of speciated Hg.

GEM oxidation is one of the main driving mechanisms of diurnal and seasonal variations of TGM/GEM and GOM. However, the oxidants that are involved in the photochemical reactions driving the diurnal and seasonal variations of GOM remain largely unknown/uncertain, due to the lack of speciated GOM and upper air measurements. This is largely a result of inadequate technologies and a nebulous understanding of chemical reactions in atmospheric Hg transformation. Studies such as Chand et al. (2008) estimated GOM concentrations using the reaction of GEM+OH alone, and Sillman et al. (2007) reproduced observed GOM concentrations over Florida using CMAQ with gas-phase oxidation of GEM by O_3 and OH only. However, the reactions of GEM+O_3 and GEM+OH have been subject to debate between theoretical and experimental studies, as no mechanism consistent with thermochemistry has been proposed (Pal and Ariya, 2004; Calvert and Lindberg, 2005; Subir et al., 2011; Ariya et al., 2015). It was speculated that GEM oxidation in the MBL and the upper troposphere was possibly largely Br-initiated (Holmes et al., 2009; Gratz et al., 2015; Shah et al., 2016). This indicated that even if a model reproduced observed concentrations of GOM, the chemistry in the model was not necessarily correct. So far, most chemical transport models have rarely focused on diurnal variation of speciated Hg; instead, they mostly focused on reproducing annual and monthly variations in TGM/GEM (Lei et al., 2013; Song et al., 2015), with large discrepancies between model simulations and surface measurements of GOM and PBM (Zhang et al., 2012; Kos et al., 2013). There are too many misrepre-

sentations of Hg science and confounding issues in current models to gain a full understanding of the driving mechanisms for the observed diurnal to decadal variation in speciated Hg.

In examining these unresolved questions and issues, the following recommendations for future research were hence suggested:

- Global tropospheric distributions need to be mapped out for TGM/GEM, GOM, and PBM. Long-term monitoring of atmospheric Hg will need to be continued in time and space, particularly over oceans and at high altitudes utilizing innovative platforms, which undoubtedly demands technological breakthroughs in instrumentation.
- Future research is warranted on GOM speciation measurements and multiphase redox kinetics. Field measurement studies need to include more oxidants besides ozone (and BrO in limited number of studies) in the analysis of diurnal variation.
- Monitoring of long-term trends in TGM/GEM needs to continue, and more work is needed to unravel the causes responsible for the observed trends. Current hypotheses need to be validated using more extensive, longer datasets and a modeling system that includes realistic representation of dynamical, physical, and chemical processes in Hg cycling not only in the atmosphere but also in the ocean and between the two systems.
- Size-fractionated PBM measurements are needed, including Hg concentrations on particles of all sizes, in space and time concurrent with TGM/GEM and GOM measurements.

7 Data availability

This is a review paper. All data are from the literature. Hence, we did not provide access to the data. All data used in the figures are provided in the tables.

The Supplement related to this article is available online at doi:10.5194/acp-16-12897-2016-supplement.

Acknowledgements. The authors acknowledge the field technicians, students and/or researchers for collection of speciated atmospheric mercury data that are summarized and discussed in this review paper. Part of this work was funded by the Environmental Protection Agency grant agreement no. 83521501. We thank Y. Zhou for her help with Fig. S1.

Edited by: R. Ebinghaus
Reviewed by: two anonymous referees

References

Abbott, M. L., Lin, C. J., Martian, P., and Einerson, J. J.: Atmospheric mercury near Salmon Falls creek reservoir in southern Idaho, Appl. Geochem., 23, 438–453, 2008.

Amos, H. M., Jacob, D. J., Kocman, D., Horowitz, H. M., Zhang, Y., Dutkiewicz, S., Horvat, M., Corbitt, E. S., Krabbenhoft, D. P., and Sunderland, E. M.: Global biogeochemical implications of mercury discharges from rivers and sediment burial, M., Environ. Sci. Technol., 48, 9514–9522, doi:10.1021/es502134t, 2014.

Angot, H., Barret, M., Magand, O., Ramonet, M., and Dommergue, A.: A 2-year record of atmospheric mercury species at a background Southern Hemisphere station on Amsterdam Island, Atmos. Chem. Phys., 14, 11461–11473, doi:10.5194/acp-14-11461-2014, 2014.

Ariya, P. A., Amyot, M., Dastoor, A., Deeds, D., Feinberg, A., Kos, G., Poulain, A., Ryjkov, A., Semeniuk, K., Subir, M., and Toyota, K.: Mercury physicochemical and biogeochemical transformation in the atmosphere and at atmospheric interfaces: a review and future directions, Chem. Rev., 115, 3760–3802, doi:10.1021/cr500667e, 2015.

Aspmo, K., Temme, C., Berg, T., Ferrari, C., Gauchard, P.-A., Fain, X., and Wibetoe, G.: Mercury in the atmosphere, snow, and melt water ponds in the North Atlantic Ocean during Arctic Summer, Environ. Sci. Technol., 40, 4083–4089, 2006.

Bagnato, E., Sproverie, M., and Barra, M.: The sea–air exchange of mercury (Hg) in the marine boundary layer of the Augusta basin (southern Italy): Concentrations and evasion flux, Chemosphere, 93, 2024–2032, 2013.

Banic, C. M., Beauchamp, S. T., Tordon, R. J., Schroeder, W. H., Steffen, A., Anlauf, K. A., and Wong, H. K. T.: Vertical distribution of gaseous elemental mercury in Canada, J. Geophys. Res., 108, 4264, doi:10.1029/2002JD002116, 2003.

Beldowska, M., Saniewska, D., Falkowska, L., and Lewandowska, A.: Mercury in particulate matter over Polish zone of the southern Baltic Sea, Atmos. Environ., 46, 397–404, 2012.

Berg, T., Pfaffhuber, K. A., Cole, A. S., Engelsen, O., and Steffen, A.: Ten-year trends in atmospheric mercury concentrations, meteorological effects and climate variables at Zeppelin, Ny-Ålesund, Atmos. Chem. Phys., 13, 6575–6586, doi:10.5194/acp-13-6575-2013, 2013.

Brooks, S., Ren, X., Cohen, M., Luke, W. T., Kelley, P., Artz, R., Hynes, A., Landing, W., and Martos, B.: Airborne Vertical Profiling of Mercury Speciation near Tullahoma, TN, USA, Atmos., 5, 557–574, doi:10.3390/atmos5030557, 2014.

Brown, R. J., Goddard, S. L., Butterfield, D. M., Brown, A. S., Robins, C., Mustoe, C. L., and McGhee, E. A.: Ten years of mercury measurement at urban and industrial air quality monitoring stations in the UK, Atmos. Environ., 109, 1–8, 2015.

Brunke, E.-G., Labuschagne, C., Ebinghaus, R., Kock, H. H., and Slemr, F.: Gaseous elemental mercury depletion events observed at Cape Point during 2007–2008, Atmos. Chem. Phys., 10, 1121–1131, doi:10.5194/acp-10-1121-2010, 2010.

Bullock, O. R. and Brehme, K. A.: Atmospheric mercury simulation using the CMAQ model: formulation description and analysis of wet deposition results, Atmos. Environ., 36, 2135–2146, 2002.

Calvert, J. G. and Lindberg, S. E.: Mechanisms of mercury removal by O3 and OH in the atmosphere, Atmos. Environ., 39, 3355–3367, 2005.

Chand, D., Jaffe, D., Prestbo, E., Swartzendruber, P. C., Hafner, W., Weiss-Penzias, P., Kato, S., Takami, A., Hatakeyama, S., and Kajii, Y.: Reactive and particulate mercury in the Asian marine boundary layer, Atmos. Environ., 28, 7988–7996, doi:10.1016/j.atmosenv.2008.06.048, 2008.

Chen, L., Liu, M., Xu, Z., Fan, R., Tao, J., Chen, D., Zhang, D., Xie, D. and Sun, J.: Variation trends and influencing factors of total gaseous mercury in the Pearl River Delta – A highly industrialised region in South China influenced by seasonal monsoons, Atmos. Environ., 77, 757–766, 2013.

Cheng, I., Zhang, L., Blanchard, P., Graydon, J. A., and Louis, V. L. St.: Source-receptor relationships for speciated atmospheric mercury at the remote Experimental Lakes Area, northwestern Ontario, Canada, Atmos. Chem. Phys., 12, 1903–1922, doi:10.5194/acp-12-1903-2012, 2012.

Choi, E. M., Kim, S. H., Holsen, T. M., and Yi, S. M.: Total gaseous concentrations in mercury in Seoul, Korea: local sources compared to long-range transport from China and Japan, Environ. Pollut., 157, 816–822, 2009.

Choi, H. D., Holsen, T. M., and Hopke, P. K.: Atmospheric mercury (Hg) in the Adirondacks: Concentrations and sources, Environ. Sci. Technol., 42, 5644–5653, 2008.

Choi, H. D., Huang, J., Mondal, S., and Holsen, T. M.: Variation in concentrations of three mercury (Hg) forms at a rural and a suburban site in New York State, Sci. Total Environ., 448, 96–106, 2013.

Ci, Z. J., Zhang, X. S., Wang, Z. W., Niu, Z. C., Diao, X. Y., and Wang, S. W.: Distribution and air-sea exchange of mercury (Hg) in the Yellow Sea, Atmos. Chem. Phys., 11, 2881–2892, doi:10.5194/acp-11-2881-2011, 2011.

Civerolo, K. L., Rattigan, O. V., Felton, H. D., Hirsch, M. J., and DeSantis, S.: Mercury wet deposition and speciated air concentrations from two urban sites in New York State: Temporal patterns and regional context, Aerosol Air Qual. Res., 14, 1822–1837, 2014.

Cobbett, F. D. and Van Heyst, B. J.: Measurements of GEM fluxes and atmospheric mercury concentrations (GEM, RGM and Hgp) from an agricultural field amended with biosolids in Southern Ont., Canada (October 2004–November 2004), Atmos. Environ., 41, 2270–2282, 2007.

Cole, A. S., Steffen, A., Pfaffhuber, K. A., Berg, T., Pilote, M., Poissant, L., Tordon, R., and Hung, H.: Ten-year trends of atmospheric mercury in the high Arctic compared to Canadian sub-Arctic and mid-latitude sites, Atmos. Chem. Phys., 13, 1535–1545, doi:10.5194/acp-13-1535-2013, 2013.

Cole, A. S., Steffen, A., Eckley, C. S., Narayan, J., Pilote, M., Tordon, R., Graydon, J. A., St. Louis, V.L., Xu, X., and Branfireun, B. A.: A survey of mercury in air and precipitation across Canada: patterns and trends, Atmosphere, 5, 635–668, 2014.

Conaway, C. H., Mason, R. P., Steding, D. J., and Flegal, A. R.: Estimate of mercury emission from gasoline and diesel fuel consumption, San Francisco Bay area, California, Atmos. Environ., 39, 101–105, 2005.

Dastoor, A. P. and Durnford, D. A.: Arctic Ocean: is it a sink of a source of atmospheric mercury?, Environ. Sci. Technol., 48, 1707–1717, 2014.

De More, S. J., Patterson, J. E., and Bibby, D. M.: Baseline atmospheric mercury studies at Ross Island, Antarctica, Antarctic Sci., 5, 323–326, 1993.

Dibble, T. S., Zelie, M. J., and Mao, H.: Thermodynamics of reactions of ClHg and BrHg radicals with atmospherically abundant free radicals, Atmos. Chem. Phys., 12, 10271–10279, doi:10.5194/acp-12-10271-2012, 2012.

Driscoll, C. T., Mason, R. P., Chan, H. M., Jacob, D. J., and Pirrone, N.: Mercury as a global pollutant: sources, pathways, and effect, Environ. Sci. Technol., 47, 4967–4983, 2013.

Ebinghaus, R. and Slemr, F.: Aircraft measurements of atmospheric mercury over southern and eastern Germany, Atmos. Environ., 34, 895–903, 2000.

Ebinghaus, R., Kock, H. H., Coggin, A. M., Spain, T. G., Jennings, S. G., and Temme, C.: Long term measurements of atmospheric mercury at Mace Head, Irish west coast, between 1995 and 2001, Atmos. Environ., 36, 5267–5276, 2002a.

Ebinghaus, R., Kock, H. H., Temme, C., Einax, J. W., Löwe, A. G., Richter, A., Burrows, J. P., and Schroeder, W. H.: Antarctic springtime depletion of atmospheric mercury, Environ. Sci. Technol., 36, 1238–1244, 2002b.

Ebinghaus, R., Slemr, F., Brenninkmeijer, C. A. M., van Velthoven, P., Zahn, A., Hermann, M., O'Sullivan, D. A., and Oram, D. E.: Emissions of gaseous mercury from biomass burning in South America in 2005 observed during CARIBIC flights, Geophys. Res. Lett., 34, L08813, doi:10.1029/2006GL028866, 2007.

Ebinghaus, R., Jennings, S. G., Kock, H. H., Derwent, R. G., Manning, A. J., and Spain, T. G.: Decreasing trends in total gaseous mercury observations in baseline air at Mace Head, Ireland from 1996 to 2009, Atmos. Environ., 45, 3475–3480, 2011.

Eckley, C. S., Parsons, M. T., Mintz, R., Lapalme, M., Mazur, M., Tordon, R., Elleman, R., Graydon, J. A., Blanchard, P., and St. Louis, V.: Impact of closing Canada's largest point-source of mercury emissions on local atmospheric mercury concentrations, Environ. Sci. Technol., 47, 10339–10348, 2013.

Engle, M. A., Tate, M. T., Krabbenhoft, D. P., Schauer, J. J., Kolker, A., Shanley, J. B., and Bothner, M. H.: Comparison of atmospheric mercury speciation and deposition at nine sites across central and eastern North America, J. Geophys. Res.-Atmos., 115, doi:10.1029/2010JD014064, 2010.

Faïn, X., Obrist, D., Hallar, A. G., Mccubbin, I., and Rahn, T.: High levels of reactive gaseous mercury observed at a high elevation research laboratory in the Rocky Mountains, Atmos. Chem. Phys., 9, 8049–8060, doi:10.5194/acp-9-8049-2009, 2009.

Feddersen, D. M., Talbot, R., Mao, H., and Sive, B. C.: Size distribution of particulate mercury in marine and coastal atmospheres, Atmos. Chem. Phys., 12, 10899–10909, doi:10.5194/acp-12-10899-2012, 2012.

Fitzgerald, W. F.: Is mercury increasing in the atmosphere? The need for an atmospheric mercury network (AMNET), Water Air Soil Pollut., 80, 245–254, 1995.

Fitzgerald, W. F. and Mason, R. P.: The global mercury cycle: oceanic and anthropogenic aspects, in: Global and Regional Mercury Cycles: Sources, Fluxes and Mass Balances, edited by: Baeyens, W., Ebinghaus, R., and Vasiliev, O., NATO ASI Series 2. Environment, vol. 21. Kluwer Ac. Pub., Dordrecht, 85–108, 1996.

Fitzgerald, W. F., Gill, G. A., and Kim, J. P.: An Equatorial Paci"c source of atmospheric ercury, Science, 224, 597–599, 1984.

Fostier, A. H. and Michelazzo, P. A.: Gaseous and particulate atmospheric mercury concentrations in the Campinas Metropoli-

tan Region (Sao Paulo State, Brazil), J. Brazilian Chem. Soc., 17, 886–894, 2006.

Friedli, H. R., Radke, L. F., Prescott, R., Li, P., Woo, J.-H., and Carmichael, G. R.: Mercury in the atmosphere around Japan, Korea, and China as observed during the 2001 ACE-Asia field campaign: Measurements, distributions, sources, and implications, J. Geophys. Res., 28, D19S25, doi:10.1029/2003JD004244, 2004.

Fu, X., Feng, X., Zhu, W., Wang, S., and Lu, J.: Total gaseous mercury concentrations in ambient air in the eastern slope of Mt. Gongga, South-Eastern fringe of the Tibetan plateau, China, Atmos. Environ., 42, 970–979, 2008.

Fu, X., Feng, X., Wang, S., Rothenberg, S., Shang, L., Li, Z., and Qiu, G.: Temporal and spatial distributions of total gaseous mercury concentrations in ambient air in a mountainous area in southwestern China: Implications for industrial and domestic mercury emissions in remote areas in China, Sci. Total Environ., 407, 2306–2314, 2009.

Fu, X. W., Feng, X., Dong, Z. Q., Yin, R. S., Wang, J. X., Yang, Z. R., and Zhang, H.: Atmospheric gaseous elemental mercury (GEM) concentrations and mercury depositions at a high-altitude mountain peak in south China, Atmos. Chem. Phys., 10, 2425–2437, doi:10.5194/acp-10-2425-2010, 2010a.

Fu, X., Feng, X., Zhang, G., Xu, W., Li, X., Yao, H., Liang, P., Li, J., Sommar, J., Yin, R., and Liu, N.: Mercury in the marine boundary layer and seawater of the South China Sea: Concentrations, sea/air flux, and implication for land outflow, J. Geophys. Res., 115, D06303, doi:10.1029/2009JD012958, 2010b.

Fu, X. W., Feng, X., Liang, P., Deliger, Zhang, H., Ji, J., and Liu, P.: Temporal trend and sources of speciated atmospheric mercury at Waliguan GAW station, Northwestern China, Atmos. Chem. Phys., 12, 1951–1964, doi:10.5194/acp-12-1951-2012, 2012a.

Fu, X. W., Feng, X., Shang, L. H., Wang, S. F., and Zhang, H.: Two years of measurements of atmospheric total gaseous mercury (TGM) at a remote site in Mt. Changbai area, Northeastern China, Atmos. Chem. Phys., 12, 4215–4226, doi:10.5194/acp-12-4215-2012, 2012b.

Fu, X. W., Zhang, H., Yu, B., Wang, X., Lin, C.-J., and Feng, X. B.: Observations of atmospheric mercury in China: a critical review, Atmos. Chem. Phys., 15, 9455–9476, doi:10.5194/acp-15-9455-2015, 2015.

Gratz, L. E., Keeler, G. J., Marsik, F. J., Barres, J. A., and Dvonch, J. T.: Atmospheric transport of speciated mercury across southern Lake Michigan: Influence from emission sources in the Chicago/Gary urban area, Sci. Total Environ., 448, 84–95, 2013.

Gratz, L. E., Ambrose, J. L., Jaffe, D. A., Shah, V., Jaeglé, L., Stutz, J., Festa, J., Spolaor, M., Tsai, C., Selin, N. E., and Song, S: Oxidation of mercury by bromine in the subtropical Pacific free troposphere, Geophys. Res. Lett., 42, 10494–10502, doi:10.1002/2015GL066645, 2015.

Hall, C.B., Mao, H., Ye, Z., Talbot, R., Ding, A., Zhang, Y., Zhu, J., Wang, T., Lin, C. J., Fu, C., and Yang, X.: Sources and Dynamic Processes Controlling Background and Peak Concentrations of TGM in Nanjing, China, Atmosphere, 5, 124–155, 2014.

Han, Y. J., Kim, J. E., Kim, P. R., Kim, W. J., Yi, S. M., Seo, Y. S., and Kim, S. H.: General trends of atmospheric mercury concentrations in urban and rural areas in Korea and characteristics of high-concentration events, Atmos. Environ., 94, 754–764, 2014.

Hedgecock I. M. and Pirrone, N.: Chasing quicksilver: modeling the atmospheric lifetime of Hg0 (g) in the marine boundary layer at various latitudes, Environ. Sci. Technol., 38, 69–76, 2004.

Hedgecock, I. M., Pirrone, N., Sprovieri, F., and Pesenti, E.: Reactive gaseous mercury in the marine boundary layer: Modelling and experimental evidence of its formation in the Mediterranean region, Atmos. Environ., 37, suppl. 1, S41–S49, 2003.

Hedgecock, I. M., Trunfio, G. A., Pirrone, N., and Sprovieri, F.: Mercury chemistry in the MBL: Mediterranean case and sensitivity studies using the AMCOTS (Atmospheric Mercury Chemistry over the Sea) model, Atmos. Environ., 39, 7217–7230, 2005.

Huang, J., Choi, H. D., Hopke, P. K., and Holsen, T. M.: Ambient mercury sources in Rochester, NY: results from principle components analysis (PCA) of mercury monitoring network data, Environ. Sci. Technol., 44, 8441–8445, 2010.

Holmes, C. D., Jacob, D. J., Mason, R. P., and Jaffe, D. A.: Sources and deposition of reactive gaseous mercury in the marine atmosphere, Atmos. Environ., 43, 2278–2285, 2009.

Jiang, Y., Cizdziel, J. V., and Lu, D.: Temporal patterns of atmospheric mercury species in northern Mississippi during 2011–2012: Influence of sudden population swings, Chemosphere, 93, 1694–1700, 2013.

Kang, H. and Xie, Z.: Atmospheric mercury over the marine boundary layer observed during the third China Arctic Research Expedition, J. Environ. Sci., 23, 1424–1430, 2011.

Kim, J. and Fitzgerald, W.: Gaseous mercury profiles in the tropical Pacific Ocean, Geophys. Res. Lett., 15, 40–43, 1988.

Kim, K. H., Yoon, H. O., Brown, R. J., Jeon, E. C., Sohn, J. R., Jung, K., Park, C. G., and Kim, I. S.: Simultaneous monitoring of total gaseous mercury at four urban monitoring stations in Seoul, Korea, Atmos. Res., 132, 199–208, 2013.

Kim, P. R., Han, Y. J., Holsen, T. M., and Yi, S. M.: Atmospheric particulate mercury: Concentrations and size distributions, Atmos. Environ., 61, 94–102, 2012.

Kos, G., Ryzhkov, A., Dastoor, A., Narayan, J., Steffen, A., Ariya, P. A., and Zhang, L.: Evaluation of discrepancy between measured and modelled oxidized mercury species, Atmos. Chem. Phys., 13, 4839–4863, doi:10.5194/acp-13-4839-2013, 2013.

Kotnik, J., Sprovieri, F., Ogrinc, N., Horvat, M., and Pirrone, N.: Mercury in the Mediterranean, part I: spatial and temporal trends, Environ. Sci. Pollut. Res., 21, 4063–4080, 2014.

Lamborg, C. H., Rolfhus, K. R., and Fitzgerald, W. F.: The atmospheric cycling and air-sea exchange of mercury species in the south and equatorial Atlantic Ocean, Deep Sea Res. Part II, 46, 957–977, 1999.

Lan, X., Talbot, R., Castro, M., Perry, K., and Luke, W.: Seasonal and diurnal variations of atmospheric mercury across the US determined from AMNet monitoring data, Atmos. Chem. Phys., 12, 10569–10582, doi:10.5194/acp-12-10569-2012, 2012.

Lan, X., Talbot, R., Laine, P., Lefer, B., Flynn, J., and Torres, A.: Seasonal and diurnal variations of total gaseous mercury in urban Houston, TX, USA, Atmosphere, 5, 399–419, 2014.

Landis, M. S., Lewis, C. W., Stevens, R. K., Keeler, G. J., Dvonch, J. T., and Tremblay, R. T.: Ft. McHenry tunnel study: Source profiles and mercury emissions from diesel and gasoline powered vehicles, Atmos. Environ., 41, 8711–8724, 2007.

Laurier, F. and Mason, R.: Mercury concentration and speciation in the coastal and open ocean boundary layer, J. Geophys. Res., 112, D06302, doi:10.1029/2006JD007320, 2007.

Laurier, F. J. G., Mason, R. P., Whalin, L., and Kato, S.: Reactive gaseous mercury formation in the North Pacific Ocean's marine boundary layer: A potential role of halogen chemistry, J. Geophys. Res., 108, 4529, doi:10.1029/2003JD003625, 2003.

Lei, H., Liang, X.-Z., Wuebbles, D. J., and Tao, Z.: Model analyses of atmospheric mercury: present air quality and effects of transpacific transport on the United States, Atmos. Chem. Phys., 13, 10807–10825, doi:10.5194/acp-13-10807-2013, 2013.

Li, J., Sommar, J., Wängberg, I., Lindqvist, O., and Wei, S. Q.: Short-time variation of mercury speciation in the urban of Göteborg during GÖTE-2005, Atmos. Environ., 42, 8382–8388, 2008.

Li, Z., Xia, C., Wang, X., Xiang, Y., and Xie, Z.: Total gaseous mercury in Pearl River Delta region, China during 2008 winter period, Atmos. Environ., 45, 834–838, 2011.

Lindberg, S. E., Brooks, S., Lin, C.-J., Scott, K. J., Landis, M. S., Stevens, R. K., Goodsite, M., and Richter, A.: Dynamic oxidation of gaseous mercury in the Arctic troposphere at polar sunrise, Environ. Sci. Tech., 36, 1245–1256, 2002.

Liu, B., Keeler, G. J., Dvonch, J. T., Barres, J. A., Lynam, M. M., Marsik, F. J., and Morgan, J. T.: Temporal variability of mercury speciation in urban air, Atmos. Environ., 41, 1911–1923, 2007.

Liu, B., Keeler, G. J., Dvonch, J. T., Barres, J. A., Lynam, M. M., Marsik, F. J., and Morgan, J. T.: Urban–rural differences in atmospheric mercury speciation, Atmos. Environ., 44, 2013–2023, 2010.

Lyman, S. N. and Gustin, M. S.: Speciation of atmospheric mercury at two sites in northern Nevada, USA, Atmos. Environ., 42, 927–939, 2008.

Lyman, S. N. and Gustin, M. S.: Determinants of atmospheric mercury concentrations in Reno, Nevada, USA, Sci. Total Environ., 408, 431–438, 2009.

Lyman, S. N. and Jaffe, D. A.: Formation and fate of oxidized mercury in the upper troposphere and lower stratosphere, Nature Geosci., 5, 114–117, doi:10.1038/NGEO1353, 2011.

Lynam, M. M. and Keeler, G. J.: Automated speciated mercury measurements in Michigan, Environ. Sci. Technol., 39, 9253–9262, 2005.

Manolopoulos, H., Schauer, J. J., Purcell, M. D., Rudolph, T. M., Olson, M. L., Rodger, B., and Krabbenhoft, D. P.: Local and regional factors affecting atmospheric mercury speciation at a remote location, J. Environ. Eng. Sci., 6, 491–501, 2007.

Mao, H. and Talbot, R.: Speciated mercury at marine, coastal, and inland sites in New England – Part 1: Temporal variability, Atmos. Chem. Phys., 12, 5099–5112, doi:10.5194/acp-12-5099-2012, 2012.

Mao, H., Talbot, R. W., Sigler, J. M., Sive, B. C., and Hegarty, J. D.: Seasonal and diurnal variations of Hg° over New England, Atmos. Chem. Phys., 8, 1403–1421, doi:10.5194/acp-8-1403-2008, 2008.

Mao, H., Talbot, R. W., Sive, B. C., Kim, S. Y., Blake, D. R., and Weinheimer, A. J.: Arctic mercury depletion and its quantitative link with halogens, J. Atmos. Chem., 65, 145–170, 2010.

Mao, H., Talbot, R., Hegarty, J., and Koermer, J.: Speciated mercury at marine, coastal, and inland sites in New England – Part 2: Relationships with atmospheric physical parameters, Atmos. Chem. Phys., 12, 4181–4206, doi:10.5194/acp-12-4181-2012, 2012.

Marumoto, K., Hayashi, M., and Takami, A.: Atmospheric mercury concentrations at two sites in the Kyushu Islands, Japan, and evidence of long-range transport from East Asia, Atmos. Environ., 117, 147–155, 2015.

Mason, R. P. and Sheu, G.-R.: Role of the ocean in the global mercury cycle, Global Biogeochem. Cy., 16, 1093, doi:10.1029/2001GB001440, 2002.

Mason, R. P., Lawson, N. M., and Sheu, G.-R.: Mercury in the Atlantic Ocean: factors controlling air-sea exchange of mercury and its distribution in the upper waters, Deep-Sea Res. II, 48, 2829–2853, 2001.

Mazur, M., Mintz, R., Lapalme, M., and Wiens, B.: Ambient air total gaseous mercury concentrations in the vicinity of coal-fired power plants in Alberta, Canada, Sci. Total Environ., 408, 373–381, 2009.

Moore, C., Obrist, D., and Luria, M.: Atmospheric mercury depletion events at the Dead Sea: Spatial and temporal aspects, Atmos. Environ., 69, 231–239, 2013.

Moore, C. W., Obrist, D., Steffen, A., Staebler, R. M., Douglas, T. A., Richter, A., and Nghiem, S. V.: Convective forcing ofmercury and ozone in the Arctic boundary layer induced by leads in sea ice, Nature, 506, 81–85, doi:10.1038/nature12924, 2014.

Müller, D., Wip, D., Warneke, T., Holmes, C. D., Dastoor, A., and Notholt, J.: Sources of atmospheric mercury in the tropics: continuous observations at a coastal site in Suriname, Atmos. Chem. Phys., 12, 7391–7397, doi:10.5194/acp-12-7391-2012, 2012.

Murphy, D. M., Thomson, D. S., and Mahoney, M. J.: In situ measurements of organics, meteoritic material, mercury, and other elements in aerosols at 5 to 19 kilometers, Science, 282, 1664–1669, 1998.

Murphy, D. M., Hudson, P. K., Thomson, D. S., Sheridan, P. J., and Wilson, J. C.: Observations of mercury-containing aerosols, Environ. Sci. Technol., 40, 3163–3167, 2006.

Nair, U. S., Wu, Y., Walters, J., Jansen, J., and Edgerton, E. S.: Diurnal and seasonal variation of mercury species at coastal-suburban, urban, and rural sites in the southeastern United States, Atmos. Environ., 47, 499–508, 2012.

Nguyen, D. L., Kim, J. Y., Shim, S. G., and Zhang, X. S.: Ground and shipboard measurements of atmospheric gaseous elemental mercury over the Yellow Sea region during 2007–2008, Atmos. Environ., 45, 253–260, 2011.

Obrist, D., Hallar, A. G., McCubbin, I., Stephens, B. B., and Rahn, T.: Atmospheric mercury concentrations at Storm Peak Laboratory in the Rocky Mountains: Evidence for long-range transport from Asia, boundary layer contributions, and plant mercury uptake, Atmos. Environ., 42, 7579–7589, 2008.

Obrist, D., Tas, E., Peleg, M., Matveev, V., Faïn, X., Asaf, D., and Lur, M.: Bromine-induced oxidation of mercury in the mid-latitude atmosphere, Nature Geosci., 4, 22–26, 2011.

Pal, B. and Ariya, P. A.: Gas-phase HO-initiated reactions of elemental mercury: kinetics, product studies, and atmospheric implications, Environ. Sci. Technol., 38, 5555–5566, 2004.

Parsons, M. T., McLennan, D., Lapalme, M., Mooney, C., Watt, C., and Mintz, R.: Total gaseous mercury concentration measurements at Fort McMurray, Alberta, Canada, Atmosphere, 4, 472–493, 2013.

Peterson, C., Gustin, M., and Lyman, S.: Atmospheric mercury concentrations and speciation measured from 2004 to 2007 in Reno, Nevada, USA, Atmos. Environ., 43, 4646–4654, 2009.

Pfaffhuber, K. A., Berg, T., Hirdman, D., and Stohl, A.: Atmospheric mercury observations from Antarctica: seasonal variation and source and sink region calculations, Atmos. Chem. Phys., 12, 3241–3251, doi:10.5194/acp-12-3241-2012, 2012.

Pirrone, N., Ferrara, R., Hedgecock, I. M., Kallos, G., Mamane, Y., Munthe, J., Pacyna, J. M., Pytharoulis, I., Sprovieri, F., Voudouri, A., and Wangberg, I.: Dynamic processes of atmospheric mercury over the Mediterranean region, Atmos. Environ., 37, 21–40, 2003.

Pirrone, N., Cinnirella, S., Feng, X., Finkelman, R. B., Friedli, H. R., Leaner, J., Mason, R., Mukherjee, A. B., Stracher, G. B., Streets, D. G., and Telmer, K.: Global mercury emissions to the atmosphere from anthropogenic and natural sources, Atmos. Chem. Phys., 10, 5951–5964, doi:10.5194/acp-10-5951-2010, 2010.

Prestbo, E. M.: Mercury speciation in the boundary layer and free troposphere advected to South Florida: Phase I – Reconnaissance, Report to the Florida Department of Environmental Protection, Tallahassee, Frontier Geosciences, Seattle, WA, 1997.

Radke, L. F., Friedli, H. R., and Heikes, B. G.: Atmospheric mercury over the NE Pacific during spring 2002: Gradients, residence time, upper troposphere lower stratosphere loss, and long-range transport, J. Geophys. Res., 112, D19305, doi:10.1029/2005JD005828, 2007.

Rothenberg, S. E., McKee, L., Gilbreath, A., Yee, D., Connor, M., and Fu, X.: Evidence for short-range transport of atmospheric mercury to a rural, inland site, Atmos. Environ., 44, 1263–1273, 2010.

Rutter, A. P. and Schauer, J. J.: The effect of temperature on the gas–particle partitioning of reactive mercury in atmospheric aerosols, Atmos. Environ., 41, 8647–8657, 2007.

Rutter, A. P., Schauer, J. J., Lough, G. C., Snyder, D. C., Kolb, C. J., Von Klooster, S., Rudolf, T., Manolopoulos, H., and Olson, M. L.: A comparison of speciated atmospheric mercury at an urban center and an upwind rural location, J. Environ. Monit., 10, 102–108, 2008.

Schleicher, N. J., Schafer, J., Blanc, G., Chen, Y., Chai, F., Cen, K., and Norra, S.: Atmospheric particulate mercury in the megacity Beijing: Spatiotemporal variations and source apportionment, Atmos. Environ., 109, 251–261, 2015.

Schroeder, W. H. and Munthe, J.: Atmospheric mercury – an overview, Atmos. Environ., 32, 809–822, 1998.

Schroeder, W. H., Anlauf, K. G., Barrie, L. A., Lu, J. Y., Steffen, A., Schneeberger, D. R., and Berg, T.: Arctic springtime depletion of mercury, Nature, 394, 331–332, 1998.

Seiler, W., Eberling, C., and Slemr, G.: Global distribution of gaseous mercury in the troposphere, Pageoph, 118, 964–974, 1980.

Selin, N. E., Jacob, D. J., Park, R. J., Yantosca, R. M., Strode, S. A., Jaegle, L., and Jaffe, D.: Chemical cycling and deposition of atmospheric mercury: Global constraints from observations, J. Geophys. Res., 112, D02308, doi:10.1029/2006JD007450, 2007.

Shah, V., Jaeglé, L., Gratz, L. E., Ambrose, J. L., Jaffe, D. A., Selin, N. E., Song, S., Campos, T. L., Flocke, F. M., Reeves, M., Stechman, D., Stell, M., Festa, J., Stutz, J., Weinheimer, A. J., Knapp, D. J., Montzka, D. D., Tyndall, G. S., Apel, E. C., Hornbrook, R. S., Hills, A. J., Riemer, D. D., Blake, N. J., Cantrell, C. A., and Mauldin III, R. L.: Origin of oxidized mercury in the summertime free troposphere over the southeastern US, Atmos. Chem. Phys., 16, 1511–1530, doi:10.5194/acp-16-1511-2016, 2016.

Sheu, G.-R.: Speciation and distribution of atmospheric mercury: Significance of reactive gaseous mercury in the global mercury cycle, Ph.D. thesis, 170 pp., Univ. of Md., College Park, 2001.

Sheu, G.-R. and Mason, R. P.: An examination of methods for the measurements of reactive gaseous mercury in the atmosphere, Environ. Sci. Technol., 35, 1209–1216, 2001.

Sheu, G.-R. and Mason, R. P.: An examination of the oxidation of elemental mercury in the presence of halide surfaces, J. Atmos. Chem., 48, 107–130, 2004.

Sheu, G. R., Lin, N. H., Wang, J. L., Lee, C. T., Yang, C. F. O., and Wang, S. H.: Temporal distribution and potential sources of atmospheric mercury measured at a high-elevation background station in Taiwan, Atmos. Environ., 44, 2393–2400, 2010.

Sigler, J. M., Mao, H., and Talbot, R.: Gaseous elemental and reactive mercury in Southern New Hampshire, Atmos. Chem. Phys., 9, 1929–1942, doi:10.5194/acp-9-1929-2009, 2009a.

Sigler, J. M., Mao, H., Sive, B. C., and Talbot, R.: Oceanic influence on atmospheric mercury at coastal and inland sites: a springtime noreaster in New England, Atmos. Chem. Phys., 9, 4023–4030, doi:10.5194/acp-9-4023-2009, 2009b.

Sillman, S., Marsik, F. J., Al-Wali, K. I., Keeler, G. J., and Landis, M. S.: Reactive mercury in the troposphere: Model formation and results for Florida, the northeastern United States, and the Atlantic Ocean, J. Geophys. Res.-Atmos., 112, D23305, doi:10.1029/2006JD008227, 2007.

Slemr, F.: Trends in atmospheric mercury concentrations over the Atlantic ocean and the Wank summit, and the resulting constraints on the budget of atmospheric mercury, in: Global and Regional Mercury Cycles: Sources, Fluxes and Mass Balances, edited by: Bayyens, W., Ebinghaus, R., and Vasiliev, O., NATO-ASI-Series, Vol. 21, 33–84, Kluwer Academic Publishers, Dordrecht, the Netherlands, 1996.

Slemr, F. and Langer, E.: Increase in global atmospheric concentrations of mercury inferred from measurements over the Atlantic Ocean, Nature 355, 434–437, 1992.

Slemr, F., Seiler, W., and Schuster, G.: Latitudinal distribution of mercury over the Atlantic Ocean, J. Geophys. Res., 86, 1159–1166, 1981.

Slemr, F., Schuster, G., and Seiler, W.: Distribution, speciation, and budget of atmospheric mercury, J. Atmos. Chem., 3, 407–434, 1985.

Slemr, F., Junkermann, R. W., Schmidt, W. H., and Sladkovic, R.: Indication of change in global and regional trends of atmospheric mercury concentrations, Geophys. Res. Lett., 22, 2143–2146, 1995.

Slemr, F., Brunke, E.-G., Labuschagne, C., and Ebinghaus, R.: Total gaseous mercury concentrations at the Cape Point GAW station and their seasonality, Geophys. Res. Lett., 35, L11807, doi:10.1029/2008GL033741, 2008.

Slemr, F., Brunke, E.-G., Ebinghaus, R., and Kuss, J.: Worldwide trend of atmospheric mercury since 1995, Atmos. Chem. Phys., 11, 4779–4787, doi:10.5194/acp-11-4779-2011, 2011.

Slemr, F., Angot, H., Dommergue, A., Magand, O., Barret, M., Weigelt, A., Ebinghaus, R., Brunke, E.-G., Pfaffhuber, K. A., Edwards, G., Howard, D., Powell, J., Keywood, M., and Wang, F.:

Comparison of mercury concentrations measured at several sites in the Southern Hemisphere, Atmos. Chem. Phys., 15, 3125–3133, doi:10.5194/acp-15-3125-2015, 2015.

Soerensen, A. L., Skov, H., Jacob, D. J., Soerensen, B. T., and Johnson, M. S.: Global Concentrations of Gaseous Elemental Mercury and Reactive Gaseous Mercury in the Marine Boundary Layer, Environ. Sci. Technol., 44, 7425–7430, doi:10.1021/es903839n, 2010.

Soerensen, A. L., Jacob, D. J., Streets, D. G., Witt, M. L. I., Ebinghaus, R., Mason, R. P., Andersson, M., and Sunderland, E. M.: Multi-decadal decline of mercury in the North Atlantic atmosphere explained by changing subsurface seawater concentrations, Geophys. Res. Lett., 39, L21810, doi:10.1029/2012GL053736, 2012.

Soerensen, A. L., Mason, R. P., Balcom, P. H., Jacob, D. J., Zhang, Y., Kuss, J., and Sunderland, E. M.: Elemental Mercury Concentrations and Fluxes in the Tropical Atmosphere and Ocean, Environ. Sci. Technol., 48, 11312–11319, doi:10.1021/es503109p, 2014.

Sommar, J., Andersson, M. E., and Jacobi, H.-W.: Circumpolar measurements of speciated mercury, ozone and carbon monoxide in the boundary layer of the Arctic Ocean, Atmos. Chem. Phys., 10, 5031–5045, doi:10.5194/acp-10-5031-2010, 2010.

Song, S., Selin, N. E., Soerensen, A. L., Angot, H., Artz, R., Brooks, S., Brunke, E.-G., Conley, G., Dommergue, A., Ebinghaus, R., Holsen, T. M., Jaffe, D. A., Kang, S., Kelley, P., Luke, W. T., Magand, O., Marumoto, K., Pfaffhuber, K. A., Ren, X., Sheu, G.-R., Slemr, F., Warneke, T., Weigelt, A., Weiss-Penzias, P., Wip, D. C., and Zhang, Q.: Top-down constraints on atmospheric mercury emissions and implications for global biogeochemical cycling, Atmos. Chem. Phys., 15, 7103–7125, doi:10.5194/acp-15-7103-2015, 2015.

Song, X., Cheng, I., and Lu, J.: Annual atmospheric mercury species in downtown Toronto, Canada, J. Environ. Monit., 11, 660–669, 2009.

Sprovieri, F. and Pirrone, N., Spatial and temporal distribution of atmospheric mercury species over the Adriatic Sea, Environ. Fluid Mech., 8, 117–128, doi:10.1007/s10652-007-9045-4, 2008.

Sprovieri, F., Pirrone, N., Hedgecock, I. M., Landis, M. S., and Stevens, R. K.: Intensive atmospheric mercury measurements at Terra Nova Bay in Antarctica during November and December 2000, J. Geophys. Res., 107, 4722, doi:10.1029/2002JD002057, 2002.

Sprovieri, F., Pirrone, N., Gärfeldt, K., and Sommar, J.: Mercury measurements in the marine boundary layer along a 6000 km cruise path around the Mediterranean Sea, Atmos. Environ., 37 suppl., S63–S71, 2003.

Sprovieri, F., Hedgecock, I. M., and Pirrone, N.: An investigation of the origins of reactive gaseous mercury in the Mediterranean marine boundary layer, Atmos. Chem. Phys., 10, 3985–3997, doi:10.5194/acp-10-3985-2010, 2010a.

Sprovieri, F., Pirrone, N., Ebinghaus, R., Kock, H., and Dommergue, A.: A review of worldwide atmospheric mercury measurements, Atmos. Chem. Phys., 10, 8245–8265, doi:10.5194/acp-10-8245-2010, 2010b.

Stamenkovic, J., Lyman, S., and Gustin, M. S.: Seasonal and diel variation of atmospheric mercury concentrations in the Reno (Nevada, USA) airshed, Atmos. Environ., 41, 6662–6672, 2007.

Steffen, A., Douglas, T., Amyot, M., Ariya, P., Aspmo, K., Berg, T., Bottenheim, J., Brooks, S., Cobbett, F., Dastoor, A., Dommergue, A., Ebinghaus, R., Ferrari, C., Gardfeldt, K., Goodsite, M. E., Lean, D., Poulain, A. J., Scherz, C., Skov, H., Sommar, J., and Temme, C.: A synthesis of atmospheric mercury depletion event chemistry in the atmosphere and snow, Atmos. Chem. Phys., 8, 1445–1482, doi:10.5194/acp-8-1445-2008, 2008.

Steffen, A., Bottenheim, J., Cole, A., Douglas, T. A., Ebinghaus, R., Friess, U., Netcheva, S., Nghiem, S., Sihler, H., and Staebler, R.: Atmospheric mercury over sea ice during the OASIS-2009 campaign, Atmos. Chem. Phys., 13, 7007–7021, doi:10.5194/acp-13-7007-2013, 2013.

Strode, S. A., Jaegle, L., Selin, N. E., Jacob, D. J., Park, R. J., Yantosca, R. M., Mason, R. P., and Slemr, F.: Air-sea exchange in the global mercury cycle, Global Biogeochem. Cy., 21, GB1017, doi:10.1029/2006GB002766, 2007.

Subir, M., Ariya, P. A., and Dastoor, A. P.: A review of uncertainties in atmospheric modeling of mercury chemistry I. Uncertainties in existing kinetic parameters – fundamental limitations and the importance of heterogeneous chemistry, Atmos. Environ., 45, 5664–5676, 2011.

Swartzendruber, P. C., Jaffe, D. A., Prestbo, E. M., Weiss-Penzias, P., Selin, N. E., Park, R., Jacob, D. J., Strode, S., and Jaegle, L.: Observations of reactive gaseous mercury in the free troposphere at the Mount Bachelor Observatory, J. Geophys. Res.-Atmos., 111, D24301, doi:10.1029/2006JD007415, 2006.

Swartzendruber, P. C., Chand, D., Jaffe, D. A., Smith, J., Reidmiller, D., Gratz, L., Keeler, J., Strode, S., Jaegle, L., and Talbot, R.: Vertical distribution of mercury, CO, ozone, and aerosol scattering coefficient in the Pacific Northwest during the spring 2006 INTEX-B campaign, J. Geophys. Res., 113, D10305, doi:10.1029/2007JD009579, 2008.

Talbot, R., Mao, H., Scheuer, E., Dibb, J., and Avery, M.: Total Depletion of Hg° in the Upper Troposphere – Lower Stratosphere, Geophys. Res. Lett., 34, L23804, doi:10.1029/2007GL031366, 2007.

Talbot, R., Mao, H., Scheuer, E., Dibb, J., Avery, M., Browell, E., Sachse, G., Vay, S., Blake, D., Huey, G., and Fuelberg, H.: Factors influencing the large-scale distribution of Hg° in the Mexico City area and over the North Pacific, Atmos. Chem. Phys., 8, 2103–2114, doi:10.5194/acp-8-2103-2008, 2008.

Temme, C., Slemr, F., Ebinghaus, R., and Einax, J. W.: Distribution of mercury over the Atlantic Ocean in 1996 and 1999–2001, Atmos. Environ., 37, 1889–1897, 2003a.

Temme, C., Einax, J. W., Ebinghaus, R., and Schroeder, W. H.: Measurements of mercury species at a coastal site in the Antarctic and over the South Atlantic Ocean in the polar summer, Environ. Sci. Technol., 37, 22–31, 2003b.

Timonen, H., Ambrose, J. L., and Jaffe, D. A.: Oxidation of elemental Hg in anthropogenic and marine airmasses, Atmos. Chem. Phys., 13, 2827–2836, doi:10.5194/acp-13-2827-2013, 2013.

Tseng, C. M., Liu, C. S., and Lamborg, C.: Seasonal changes in gaseous elemental mercury in relation to monsoon cycling over the northern South China Sea, Atmos. Chem. Phys., 12, 7341–7350, doi:10.5194/acp-12-7341-2012, 2012.

UNEP, Global Mercury Assessment 2013: Sources, Emissions, Releases and Environmental Transport, UNEP Chemicals Branch, Geneva, Switzerland, 2013.

Wan, Q., Feng, X., Lu, J., Zheng, W., Song, X., Han, S., and Xu, H.: Atmospheric mercury in Changbai Mountain area, northeastern China I. The seasonal distribution pattern of total gaseous mercury and its potential sources, Environ. Res., 109, 201–206, 2009a.

Wan, Q., Feng, X., Lu, J., Zheng, W., Song, X., Li, P., Han, S., and Xu, H.: Atmospheric mercury in Changbai Mountain area, northeastern China II. The distribution of reactive gaseous mercury and particulate mercury and mercury deposition fluxes, Environ. Res., 109, 721–727, 2009b.

Wang, F., Saiz-Lopez, A., Mahajan, A. S., Gómez Martín, J. C., Armstrong, D., Lemes, M., Hay, T., and Prados-Roman, C.: Enhanced production of oxidised mercury over the tropical Pacific Ocean: a key missing oxidation pathway, Atmos. Chem. Phys., 14, 1323–1335, doi:10.5194/acp-14-1323-2014, 2014.

Wang, Y., Huang, J., Hopke, P. K., Rattigan, O. V., Chalupa, D. C., Utell, M. J., and Holsen, T. M.: Effect of the shutdown of a large coal-fired power plant on ambient mercury species, Chemosphere, 92, 360–367, 2013.

Weigelt, A., Ebinghaus, R., Manning, A. J., Derwent, R. G., Simmonds, P. G., Spain, T. G., Jennings, S. G., and Slemr, F.: Analysis and interpretation of 18 years of mercury observations since 1996 at Mace Head at the Atlantic Ocean coast of Ireland, Atmos. Environ., 100, 85–93, 2015.

Weiss-Penzias, P., Jaffe, D. A., McClintick, A., Presbo, E. M., and Landis, M. S.: Gaseous elemental mercury in the Marine Boundary Layer: Evidence for rapid removal in anthropogenic pollution, Environ. Sci. Technol., 37, 3755–3763, 2003.

Weiss-Penzias, P. S., Williams, E. J., Lerner, B. M., Bates, T. S., Gaston, C., Prather, K., Vlasenko, A., and Li, S. M.: Shipboard measurements of gaseous elemental mercury along the coast of Central and Southern California, J. Geophys. Res.-Atmos., 118, 208–219, doi:10.1029/2012JD018463, 2013.

Weiss-Penzias, P., Jaffe, D., Swartzendruber, P., Hafner, W., Chand, D., and Prestbo, E.: Quantifying Asian and biomass burning sources of mercury using the Hg/CO ratio in pollution plumes observed at the Mount Bachelor Observatory, Atmos. Environ., 41, 4366–4379, 2007.

Weiss-Penzias, P., Gustin, M. S., and Lyman, S. N.: Observations of speciated atmospheric mercury at three sites in Nevada: Evidence for a free tropospheric source of reactive gaseous mercury, J. Geophys. Res.-Atmos., 114, doi:10.1029/2008JD011607, 2009.

Weiss-Penzias, P., Amos, H. M., Selin, N. E., Gustin, M. S., Jaffe, D. A., Obrist, D., Sheu, G.-R., and Giang, A.: Use of a global model to understand speciated atmospheric mercury observations at five high-elevation sites, Atmos. Chem. Phys., 15, 1161–1173, doi:10.5194/acp-15-1161-2015, 2015.

Weiss-Penzias, P. S., Gay, D. A., Brigham, M. E., Parsons, M. T., Gustin, M. S., and ter Schure, A.: Trends in mercury wet deposition and mercury air concentrations across the US and Canada, Sci. Total Environ., 568, 546–556, doi:10.1016/j.scitotenv.2016.01.061, 2016.

Williston, S. H.: Mercury in the atmosphere, J. Geophys. Res., 73, 7051–7055, doi:10.1029/JB073i022p07051, 1968.

Witt, M. L. I., Mather, T. A., Baker, A. R., De Hoog, J. C. M., and Pyle, D. M.: Atmospheric trace metals over the south-west Indian Ocean: total gaseous mercury, aerosol trace metal concentrations and lead isotope ratios, Mar. Chem., 121, 2–16, 2010a.

Witt, M. L. I., Meheran, N., Mather, T. A., De Hoog, J. C. M., and Pyle, D. M.: Aerosol trace metals, particle morphology and total gaseous mercury in the atmosphere of Oxford, UK, Atmos. Environ., 44, 1524–1538, 2010b.

Won, J. H., Park, J. Y., and Lee, T. G., Mercury emissions from automobiles using gasoline, diesel, and LPG, Atmos. Environ., 41, 7547–7552, 2007.

Xia, C., Xie, Z., and Sun, L.: Atmospheric mercury in the marine boundary layer along a cruise path from Shanghai, China to Prydz Bay, Antarctica, Atmos. Environ., 44, 1815–1821, 2010.

Xiu, G., Cai, J., Zhang, W., Zhang, D., Büeler, A., Lee, S., Shen, Y., Xu, L., Huang, X., and Zhang, P.: Speciated mercury in size-fractionated particles in Shanghai ambient air, Atmos. Environ., 43, 3145–3154, 2009.

Xu, L., Chen, J., Yang, L., Niu, Z., Tong, L., Yin, L., and Chen, Y.: Characteristics and sources of atmospheric mercury speciation in a coastal city, Xiamen, China, Chemosphere, 119, 530–539, 2015.

Xu, X. and Akhtar, U. S.: Identification of potential regional sources of atmospheric total gaseous mercury in Windsor, Ontario, Canada using hybrid receptor modeling, Atmos. Chem. Phys., 10, 7073–7083, doi:10.5194/acp-10-7073-2010, 2010.

Xu, X., Akhtar, U., Clark, K., and Wang, X.: Temporal variability of atmospheric total gaseous mercury in Windsor, ON, Canada, Atmosphere, 5, 536–556, 2014.

Yatavelli, R. L., Fahrni, J. K., Kim, M., Crist, K. C., Vickers, C. D., Winter, S. E., and Connell, D. P.: Mercury, PM 2.5 and gaseous co-pollutants in the Ohio River Valley region: Preliminary results from the Athens supersite, Atmos. Environ., 40, 6650–6665, 2006.

Yu, J., Xie, Z., Kang, H., Li, Z., Sun, C., Bian, L., and Zhang, P.: High variability of atmospheric mercury in the summertime boundary layer through the central Arctic Ocean, Scientific Reports, 4, 6091, doi:10.1038/srep06091, 2014.

Zhang, H., Fu, X. W., Lin, C.-J., Wang, X., and Feng, X. B.: Observation and analysis of speciated atmospheric mercury in Shangri-La, Tibetan Plateau, China, Atmos. Chem. Phys., 15, 653–665, doi:10.5194/acp-15-653-2015, 2015.

Zhang, L., Wright L. P., and Blanchard P.: A review of current knowledge concerning dry deposition of atmospheric mercury, Atmos. Environ., 43, 5853–5864, 2009.

Zhang, L., Blanchard, P., Johnson, D., Dastoor, A., Ryzhkov, A., Lin, C.-J., Vijayaraghavan, K., Gay, D., Holsen, T. M., Huang, J., Graydon, J. A., St. Louis, V. L., Castro, M. S., Miller, E. K., Marsik, F., Lu, J., Poissant, L., Pilote, M., and Zhang, K. M.: Assessment of modelled mercury deposition over the Great Lakes region, Environ. Pollut., 161, 272–283, 2012.

Zhang, L., Wang, S. X., Wang, L., and Hao, J. M.: Atmospheric mercury concentration and chemical speciation at a rural site in Beijing, China: implications of mercury emission sources, Atmos. Chem. Phys., 13, 10505–10516, doi:10.5194/acp-13-10505-2013, 2013.

Zhang, Y., Jacob, D. J., Horowitz, H. M., Chen, L., Amos, H. M., Krabbenhoft, D. P., Slemr, F., St. Louis, V. L., and Sunderland, E. M.: Observed decrease in atmospheric mercury explained by global decline in anthropogenic emissions, P. Natl. Acad. Sci., 113, 526–531, 2016.

Zhu, J., Wang, T., Talbot, R., Mao, H., Hall, C. B., Yang, X., Fu, C., Zhuang, B., Li, S., Han, Y., and Huang, X.: Characteris-

tics of atmospheric Total Gaseous Mercury (TGM) observed in urban Nanjing, China, Atmos. Chem. Phys., 12, 12103–12118, doi:10.5194/acp-12-12103-2012, 2012.

Zielonka, U., Hlawiczka, S., Fudala, J., Wängberg, I., and Munthe, J.: Seasonal mercury concentrations measured in rural air in Southern Poland: Contribution from local and regional coal combustion, Atmos. Environ., 39, 7580–7586, 2005.